HERPES SIMPLEX VIRUS ICP27 PROTEIN DIRECTLY INTERACTS WITH THE NUCLEAR PORE COMPLEX THROUGH NUP62, INHIBITING HOST NUCLEOCYTOPLASMIC TRANSPORT PATHWAYS

Poonam Malik[§,¶,1], Alijan Tabarraei[¶,*], Ralph H. Kehlenbach[†], Nadia Korfali[§], Ryota Iwasawa[§,‡], Sheila V. Graham[¶,1] and Eric C. Schirmer[§]

[§] Wellcome Trust Centre for Cell Biology and Institute of Cell Biology, School of Biological Sciences, University of Edinburgh, Mayfield Road, Edinburgh, EH9 3JR, Scotland, UK; [¶] Institute of Infection, Immunity and Inflammation, College of Medical, Veterinary and Life Sciences, University of Glasgow, Glasgow, Scotland, UK; [†] Universität Göttingen, Zentrum für Biochemie und Molekulare Zellbiologie, Humboldtallee 23, 37073 Göttingen, Germany; [*] Current address: Department of Microbiology, School of Medicine, Golestan University of Medical Sciences, Infectious Disease Research Centre, Iran; [‡] Current address: Department of Medicine, Faculty of Medicine, Imperial College London, Hammersmith Campus, London UK

Running title: ICP27 interaction with Nup62

[1] Address correspondence to: **Poonam Malik,** PhD, Institute of Cell Biology, School of Biological Sciences, Centre for Translational and Chemical Biology and Centre for Infectious Diseases, Michael Swann Building, King's Buildings, University of Edinburgh, Mayfield Road, Edinburgh, EH9 3JR, Scotland, UK. Tel.: +44-131-6507095; E-mail: **p.malik@ed.ac.uk** or **Sheila V. Graham**, PhD, MRC-University of Glasgow Centre for Virus Research, Institute of Infection, Immunity and Inflammation, College of Medical, Veterinary and Life Sciences, University of Glasgow, Glasgow, G61 1QH, Scotland, UK E-mail: sheila.graham@gla.ac.uk

CAPSULE

Background
Several aspects of herpes simplexvirus ICP27-trafficking remains unclear.

Results

We investigated if ICP27 could interact with the nuclear pore complex, finding that ICP27 directly binds the core nucleoporin Nup62.

Conclusions

ICP27-association with Nup62 may provide additional binding sites at the pore for ICP27-shuttling.

Significance

We propose that ICP27 competes with some transport receptors, resulting in inhibition of host pathways and supporting ICP27-mediated transport of HSV-1 mRNAs.

ABSTRACT

The herpes simplex virus ICP27 protein is important for the expression and nuclear export of viral mRNAs. Although several binding sites have been mapped along the ICP27 sequence for various RNA and protein partners including the transport receptor TAP of the host cell nuclear transport machinery, several aspects of ICP27 trafficking through the nuclear pore complex remain unclear. We investigated if ICP27 could interact directly with the nuclear pore complex itself, finding that ICP27 directly binds the core nucleoporin Nup62. This is confirmed through co-immunoprecipitation and *in vitro* binding assays with purified components. Mapping with ICP27 deletion and point mutants further shows that the interaction requires sequences in both the N- and C-termini of ICP27. Expression of wild-type ICP27 protein inhibited both classical, importin α/β-dependent and transportin-dependent nuclear import. In contrast, an ICP27 point mutant that does not interact with Nup62 had no such inhibitory effect. We suggest that ICP27 association with Nup62 provides additional binding sites at the nuclear pore for ICP27 shuttling thus supporting ICP27-mediated transport. We propose that ICP27 competes with some host cell transport receptors for binding, resulting in inhibition of those host transport pathways.

INTRODUCTION

Herpesvirus replication involves a highly regulated temporal cascade of gene expression that depends greatly on the host cell nuclear pore complex (NPC)[2] (1). Initially, the NPC is used for nuclear import of the viral genome (2). Then, when the virus lytic infection cycle proceeds, immediate early herpesvirus mRNAs are exported from the nucleus to make the immediate early-proteins in the cytoplasm that must be imported into the nucleus to activate the early genes that in turn are exported as mRNAs to make the early proteins, and this cycle repeats again for late genes and the late proteins (reviewed in 3).

The NPCs are the cellular mediators of transport in and out of the nucleus, assembled from multiple copies of over 30 different nucleoporin (Nup) proteins (4). Transport of macromolecules through the NPC is typically mediated by transport receptors that bind/coat the cargo and interact with Nups to negotiate the central channel of the NPC (reviewed in 5). Binding of transport receptors to cargos for nuclear import is signal sequence-mediated (reviewed in 6). Import receptors such as importin/karyopherin ß bind to classical basic nuclear localization signals (NLSs) (6). Some viral and cellular factors known to be involved in transport interact with a variety of transport receptors to facilitate recycling of proteins through the NPC. Human immunodeficiency virus (HIV-1) Rev protein interacts with multiple transport receptors including importin ß, transportin, importin 5 and importin 7 (7). Similarly, several ribonucleoproteins like hnRNP A1 are re-imported into the nucleus through binding of transportin-1 to M9 transport sequences that occur in many ribonucleoproteins. The transportin-1 uses interactions with core NPC Nups including Nup62 to mediate the translocation (8,9). CRM1 is an export receptor for some RNA substrates, but mostly for proteins that bind to CRM1 through their nuclear export signals (NESs) (10). CRM1 mediates the HIV-1 Rev shuttling via recognizing the Rev NES and binding to the NPC (10,11). TAP is the major cellular transport receptor for export of mRNAs (12,13). TAP-mediated transport is usually facilitated by binding of REF/Aly to the cargo-receptor complex (14); however, TAP directly binds some viral RNA sequences like the constitutive transport element (15) of Mason-Pfizer monkey virus.

Viruses tend to evolve mechanisms to control or inactivate host cell nucleocytoplasmic transport through the NPCs. Several viruses interfere with nuclear import or export pathways via degradation and/or disruption of Nups and/or transport receptors (16-21). For example, vesicular stomatitis virus (VSV) Matrix (M) protein inhibits bulk host cell mRNA export by forming a complex with the mRNA export factor RAE1 and Nup98 (22) while influenza virus NS1 protein targets the mRNA export machinery by forming inhibitory complexes with the cellular export receptors TAP/NXF1, p15/NXT, Rae1/mrnp41, and E1B-AP5 (23). The result is the same, but in each case a viral-encoded protein associates with different NPC proteins to disrupt host cell transport. In other cases a core Nup is targeted for degradation e.g. poliovirus and rhinovirus inhibit nuclear import of proteins presumably by degrading Nup62 and Nup153

(17,18). Nup62 is located at the core of the NPC (24) and is directly targeted by several viruses (21,25,26). Yet other viruses provide their own transport receptors as in the case of the human T-lymphotropic virus (HTLV) Tax protein that directly interacts with Nup62 (27).

Herpes simplex virus (HSV) encodes ICP27, an immediate early protein required for expression of early and late HSV-1 gene products, particularly through enhancing the expression and export of intron-lacking herpes-encoded mRNAs (reviewed in. 28,29). ICP27 is highly conserved among herpesviruses, with at least 30% amino acid identity among the herpesviridae (ORF57 in Kaposi's Sarcoma-associated herpes virus [KSHV], Mta/SM/EB2 in EBV, UL69 in human cytomegalovirus [HCMV]). Both ICP27 and its KSHV and EBV homologues function as export factors (30,31) and are essential for virus replication (32,33). Viruses carrying mutations in ICP27 show reduced levels of viral mRNAs, are defective in viral DNA replication (34-37) and fail to efficiently suppress cellular gene expression (38).

ICP27 binds intronless HSV-1 mRNAs but not spliced viral transcripts through its RGG domain (28,29). The functions reported for ICP27 involve multiple steps of mRNA synthesis and processing, including transcription, splicing, nuclear export (28,29) and recently translation (39-41). Overall viral RNA export is strongly reduced, but not completely ablated during infection with ICP27 mutant viruses. The remaining RNA export during herpes virus infection is probably in part due to the function of adaptors SRp20 and 9G8 (42), which are serine-arginine rich (SR) proteins that control pre-mRNA splicing and can bind directly to the export receptor TAP/NXF1 (reviewed in 43). Additionally there appear to be both ICP27-dependent and -independent pathways for different herpesvirus transcripts as during viral infection the long isoform of the UL24 transcript required ICP27 for its export whereas other viral transcripts such as gC and UL42 transcripts did not (44). ICP27 effects on translation are also mRNA specific; ICP27 influences the expression of the essential HSV tegument protein and transactivator of immediate-early gene expression VP16 by inducing translation of VP16 mRNA likely at the level of initiation (41). On the other hand, polyribosomal analysis indicated that ICP27 is not required for efficient translation of two other early HSV transcripts (thymidine kinase and ICP8) (41).

A variety of interaction sites have been identified along the ICP27 protein including an N-terminal LRR domain that binds RNA polymerase II CTD and Hsc70, a middle region that binds hnRNP K, and a C-terminal domain that also binds RNA polymerase II CTD, ICP8, protein kinase CK2β and SR proteins (reviewed in 28,29). The N- and C-terminal domains of ICP27 also fold intramolecularly to bind to one another (45) and ICP27 interacts with itself to form multimers via its C-terminal domain (46). Interestingly, the RNA polymerase II binding domain overlaps with the TAP/NXF1-binding site so that ICP27 and its associated RNAs can only be exported after release from the polymerase.

ICP27 protein can shuttle in and out of the nucleus independent of viral mRNA (47,48) but ICP27 is observed primarily in the nucleus at steady state (28,29). For HSV-1 viral mRNA export, ICP27 principally operates through interactions with the host export receptor TAP/NXF1 (48) and the transport adaptor REF/Aly (47,49). Leucine-rich NES-mediated export, dependent and independent of the CRM1 export receptor has also been reported (50); however, subsequent studies using the CRM1-inhibitor leptomycin B have shown that CRM1 is not absolutely required (47-49). Moreover, in *Xenopus* oocytes in the absence of viral RNAs export of ICP27 does not require either the known TAP/NXF1 or CRM1 receptors (47). These data argue for an alternative transport route for ICP27 nucleocytoplasmic shuttling, possibly, like the HTLV Tax protein, through direct interaction with Nups (27).

To investigate an alternative mechanism of ICP27 trafficking we tested if ICP27, like Tax, could interact with Nup62. Both ICP27 and Nup62 co-immunoprecipitated with one another in HSV-1 infected cells and interacted *in vitro* using bacterially expressed tagged proteins. This interaction is RNA-independent and is conserved as it was also observed with another herpesvirus homologue. We propose that these additional binding sites at the NPC provide ICP27-bound viral mRNA-export complexes the advantage of facilitated export.

EXPERIMENTAL PROCEDURES

Cells, Infection and Viruses — HeLa cells were grown in Dulbecco's modified Eagles medium (DMEM, Invitrogen) with 10% fetal

calf serum, 50 μg/ml penicillin and 50 μg/ml streptomycin at 37°C in 5% CO_2. BHK cells were grown in Glasgow modified Eagles medium (GMEM, Gibco) supplemented with 100 units/ml penicillin, 0.01% streptomycin, 10% newborn calf serum and 10% tryptose phosphate broth. HSV-1 wild-type (WT) strain was propagated in BHK-21 cell line and ICP27 complementing cell line, BHK derived M49 (51) was used for the growth and propagation of HSV-1 ICP27 viral mutants. Complementing cell lines were cultured in DMEM supplemented with 10% FCS and 5% tryptose phosphate broth. Selection was achieved by maintaining cells in 800 μg of G418/ml and 750 μg of Zeocin/ml. Cells were infected with WT strain 17+ or KOS1.1, for infected cell lysates with ICP27 viral mutants. Strain vBSGFP27 (52) expressing GFP fused to ICP27 under its own promoter was used for imaging. Alternatively cells were infected with ICP27 null virus d27-1 (Δ27) where the ICP27 promoter and most of the gene coding sequence has been deleted (37), or ICP27 mutant strains carrying the N-terminal deletion mutants dleu (53), d1-2 (54), d2-3 (55), d3-4 and d4-5 (56), d5-6 (56) and d6-7 (55), or C-terminal point mutants M15 and M16 (57). Virus was adsorbed onto cells for one hour and incubated at 37°C. Viruses were used at multiplicity of infections (MOIs) given in the figure legends.

Plasmids — GST–ICP27 (58), GST-Nup62, GST-RaeI and GST-TAP (59) were kind gifts from Drs Steve A. Rice (University of Minnesota, Minneapolis, USA), Stuart A. Wilson (University of Sheffield, UK) and Elisa Izaurralde (Max Plank Institute, Tübingen, Germany) respectively and GST-ORF57 (30) and pCMV-10-ICP27 (60) have been described before. His-ICP27 encodes ICP27 fused to the N-terminal His tag from the pET28 vector. mRFP-ICP27 WT and M15 recombinant (ICP27 P465L:G466E) plasmids were constructed by moving the *Eco*RI/*Bam*HI insert of pEGFP-C1-ICP27 WT and M15 into the mRFP-C1 vector (R. Tsien, USA). ICP27 WT and deletion plasmids amino acids 10-512, 166-512 and 1-403 expressed from pTriEx1.1-ICP27 have been described earlier (47). The reporter plasmid Rev_{48-116}-GFP_2-cNLS (NES-GFP_2-cNLS) was described in (61). For construction of NES-GFP_2-M9, the HIV-1 Rev sequence containing the NES (amino acids 48-116) was PCR-amplified and inserted into *XhoI* and *SpeI* sites of a modified pEGFP-C1 vector coding for a GFP-GFP fusion protein with a C-terminal M9-sequence (the NLS of hnRNPA1) (62).

Cell Lysis and Fractionation — For co-immunoprecipitation experiments, total cellular protein lysates were obtained by scraping cells into NP40 lysis buffer (0.5 % NP-40, 150 mM NaCl, 50 mM Tris pH 8.0, 2 mM EDTA, 10% glycerol) with either addition of ionic detergents [0.5% sodium deoxycholate and 0.1% SDS], or mechanical shearing by passing cells through a syringe, followed by treatment in a sonibath, with fresh addition of complete mini protease inhibitor cocktail mix (Roche) and complete phosphoSTOP (Roche). Shearing was done by 10 passes through a 26 gauge needle and sonication was for 30-60 s cycles for 10 min in a sonibath and then lysates were left rotating at 4°C for 30 min for solubilization. Debris was pelleted by centrifugation at 13,000 x g for 10-30 min in a 4°C microfuge. For Western blot analysis eluted proteins were mixed with 2x SDS sample buffer while whole cell lysates were generated by scraping cells directly into 2x SDS sample buffer. In order to standardize the amount of protein added to immunoprecipitations or pull downs, cell numbers were counted and cell equivalents of total cell protein content of soluble protein extracts was determined by Bradford assay or the various fractions were compared on SDS-polyacrylamide gels and Western blotted to examine protein expression.

Western Blot Analysis And Antibodies — Proteins were fractionated by SDS-PAGE and transferred to nitrocellulose membranes. Membranes were blocked with 5% milk powder in PBS containing 0.1% Triton-X-100 (PBST) either overnight at 4°C or for 1 h. Membranes were incubated with primary Abs in the same buffer for 1-2 h at RT or overnight at 4°C, washed, and incubated with anti-mouse IgG, anti-rabbit IgG or anti-goat IgG conjugated to horseradish peroxidase for 1 h with shaking. Following washing in PBST, proteins on membranes were visualized either using ECL (GE Healthcare) and exposed to Kodak X-OMAT S film or analysed directly on a Li-COR Odyssey (Li-COR Biosciences) using antibodies conjugated to fluorescent markers. Monoclonal primary antibodies (Abs) used were against ICP27 (1119/1113, Virusys Corporation; 1:2,000), GAPDH (Cat No. 4300, Ambion; 1:10,000), His-tag (Novagen), P53 Ab (DO-1, BD Pharmingen; 1:500), PML Ab (5E10),

Nup98 (2H10, AbCam, 1:1000) and TAP/NXF1 (G-12) (sc-28377, Santa Cruz Biotechnology; 1:100). Polyclonal Abs used were against GAPDH (E1C604-1, 1:500) from Enogene and TAP/NXF1 (H-120 — sc-25768; 1:1000) and Nup62 (H-122, D-20 and N-19) from Santa Cruz Biotechnology.

Microscopy — 8×10^4 cells were grown on each 18 × 18 mm coverslip overnight, then infected with virus or mock infected for the times stated. Coverslips were washed three times with PBS and fixed with 3.7% formaldehyde for 10 min, then permeabilized with 0.2% Triton X-100 for 5 min at RT for fixation and finally washed three times with PBS. Alternatively, cells were first pre-extracted with 1% Triton X-100 in 25 mM Hepes pH 7.4, 150 mM KOAc, 15 mM NaCl, 5 mM $MgSO_4$ for images in Fig. 1 for 1 min, washed with PBS, and then fixed with formaldehyde. Coverslips were blocked with PBS containing 10-20% serum, 200 mM glycine or 5% BSA for 1 h at room temperature, then incubated with primary Abs diluted in 5% BSA or 1% calf serum in PBS for 1 h at room temperature: ICP27 (1119/1113, 1:400, Virusys Corporation), mab414 (1:500; Covance), Nup62 (N-19; 1:50, Santa Cruz Biotechnology), TAP (1:200, gift from Elisa Izaurralde). Coverslips were washed in PBS six times before incubation for 1 h with secondary Abs (Jackson Laboratories, donkey minimal cross-reactivity) diluted in 5% BSA or 1% (v/v) calf serum in PBS. After washing in PBS six times, cells were incubated with 4',6-diamidino-2-phenylindole (DAPI; 1:2000) as a nuclear stain and washed with PBS and coverslips were mounted with fluoromount G (EM Sciences) mounting medium. Images were taken using a Nikon TE2000-U microscope with a 1.45 NA 100X objective, Sedat quad filter set, PIFOC z-axis focus drive (Physik Instruments), and CoolSnapHQ High Speed Monochrome CCD camera (Photometrics) using IPLab4.0 and Metamorph acquisition software. For figure 1 image stacks (0.2 μm steps) were deconvolved using AutoquantX and all images were processed using Adobe photoshop CS2.

Co-immunoprecipitation Of Infected Cell Extracts — For immunoprecipitations, protein A/G–Sepharose beads were washed three times in NP40 lysis buffer. Beads were used to pre-clear cell lysates by incubation for 1 h at 4°C with rotation. When required mock or virus-infected cells were treated with 20 ng/ml LMB (Sigma) for 3 h prior to harvesting. Where stated cell lysates (500 μg) were RNase I-treated (100 U) prior to use by incubation for 1 h at 37°C. Cell extracts were mixed with the anti-ICP27 Abs H1119 and H1113 or anti-Nup62 Abs or negative control Abs for 2 h in binding buffer and protein A/G–Sepharose beads were added for another 2 h or overnight. The precipitates were washed five times with cold IPP150 (10 mM Tris–HCl pH 8, 150 mM NaCl, 1% Triton X-100) and eluted. Bound eluate was suspended in SDS-PAGE loading buffer, heated for 5 min and analyzed by SDS-PAGE. Western blot analysis was performed using Abs as described in the figure legends.

Protein Expression In E.coli — Expression of GST–TAP (59) and GST-ORF57 (30) recombinant proteins has been described. GST–ICP27 (58), GST–Nup62, GST-RaeI and GST alone recombinant proteins were expressed in *E.coli* BL21 cells and purified on glutathione-Sepharose beads (GE healthcare) as described (60). Histidine-tagged-ICP27 from pET-ICP27 was expressed in BL21 DE3 and purified using Talon resin (Clontech) as described (47). Fusion proteins immobilized on beads were pre-treated with 0.2 U DNase I and 0.2 μg RNase I per μl for 30 min at 20°C in 50 mM Tris-HCl pH 8.0, 5 mM $MgCl_2$, 2.5 mM $CaCl_2$, 100 mM NaCl, 5% glycerol, 1 mM DTT. Beads were washed twice with 20 mM Tris-HCl pH 7.5, 100 mM NaCl, 1 mM EDTA, 0.5% NP-40, 1 mM DTT, and blocked in the same buffer containing 10 mg/ml BSA for 30 min at 4°C. After blocking, the beads were resuspended in binding buffer containing 1 mg/ml BSA prior to use.

In Vitro Pull Down Assays — GST–Nup62 binding reactions were carried out in 500 μl of 10 mM Tris–HCl pH 8.0, 150 mM NaCl, 1% Triton X-100, 10% glycerol buffer, using 5 μg of GST-fusion protein bound to 20 μl of glutathione-Sepharose 4B, together with 100 μg of mock- or virus-infected cell lysates or 5 μg of purified His-ICP27 protein. In some experiments cell lysates were treated with 5 μg of RNase I prior to binding reactions. Proteins were eluted from the resin using elution buffer (50 mM Tris–HCl pH 8.0, 20 mM glutathione) and analyzed by SDS–PAGE.

Transient Transfection — For ectopic expression of ICP27, HeLa cells on coverslips in 24-well dishes were transiently transfected with 0.1 μg per well pCMV-10-ICP27 (tr27) using

fugene HD (Roche). Medium was replaced after 24 h. Cells were fixed 48 h after transfection and processed for immunofluorescence microscopy.

Transport Assays — To analyze inhibition of nuclear import, HeLa cells on coverslips in 24-well dishes were transiently transfected with 0.125 µg NES-GFP_2-cNLS or NES-GFP_2-M9, respectively, with or without 0.25 µg pCMV-10-ICP27 or pmRFP-C1 plasmid encoding WT ICP27 or mRFP-ICP27 M15 mutant, using Polyfect according to the instructions of the manufacturer (Qiagen). For pTriEx-ICP27 WT and deletion mutant expression cells were transfected with 0.5 µg plasmid DNA using Fugene HD (Roche). After 24 h, cells were fixed and processed for immunofluorescence microscopy, using the anti-ICP27 Ab or analyzed directly in case of mRFP tagged ICP27. Cells were analyzed by fluorescence microscopy with a Zeiss Axioskop2 microscope and AxioVision software for those in figure 8 and a Nikon TE2000-U microscope with a 1.45 NA 100X objective, Sedat quad filter set and CoolSnapHQ High Speed Monochrome CCD camera (Photometrics) using IPLab4.0 and Metamorph acquisition software for those in figure 9. Pictures were processed using Adobe Photoshop (San Jose, CA).

RESULTS

A subpopulation of ICP27 associates at the nuclear rim — ICP27 contributes to nuclear export of viral mRNAs and is known to partly colocalize with the cellular mRNA export factor TAP at early times after infection in the nucleus (48,49). Thus ICP27 co-localization with TAP and with the NPC itself was investigated. In HSV-1 infected cells, ICP27 shows largely diffuse distribution throughout the nucleoplasm with some punctate spots (63). Strong signals from the large nucleoplasmic pool of ICP27 (see below) makes it difficult to distinguish if a separate pool of ICP27 is stably associated with the NPC. Many nuclear envelope proteins including Nups and some transport receptors resist a pre-fixation extraction with detergent because of their interactions with the highly stable structures of the nuclear lamin polymer and the NPC (64,65). So detergent extraction was used to determine if a sub-population of ICP27 is stably associated with the NPC. Accordingly, in Triton-X-100 pre-extracted cells some of the nucleoplasmic free ICP27 is washed away leaving both punctate accumulations in the nucleoplasm and a clear rim at the nuclear periphery (Fig. 1A). This peripheral pool of ICP27 co-localizes (yellow) at the rim with FxFG nucleoporins stained with mab414 that recognizes several nucleoporins including Nup62, 98, 153 and 214, based on their unique O-linked glycosylation. Co-localization is observed at 8 and 16 h post-infection, but not visible at 4 h post-infection (Fig. 1A).

TAP that also stably associates with the NPC has a significant nucleoplasmic pool, like ICP27, that is mostly washed away by the triton pre-fixation extraction (data not shown). The remaining TAP protein co-localizes with ICP27 at the nuclear periphery (Fig. 1B). Notably, the distinct nucleoplasmic pool of ICP27 did not colocalize with TAP. This internal ICP27 could be associated with viral replication centers, indicating that there are at least three distinct subpopulations of ICP27 during virus infection: nucleoplasmic extractable, nucleoplasmic resistant, and peripheral resistant. The significant amount of ICP27 remaining associated in close proximity of the NPC is consistent with expectations that ICP27 actively shuttles and/or remains associated with viral transcripts during transport.

ICP27 protein export in the absence of viral RNA requires neither TAP nor CRM1 as use of constitutive transport element RNA or NES conjugates to block the TAP and CRM1 pathways respectively did not inhibit cytoplasmic accumulation of ICP27 when re-import of ICP27 was inhibited (47). Thus an alternative route for export must exist. We postulated that the ICP27 that resisted Triton extraction might indicate an alternative route involving direct interactions with core structural components of the NPC. In keeping with both poliovirus and HTLV proteins that interact directly with Nup62, a core structural component of the NPC central channel, we chose to test for possible interactions of ICP27 with Nup62. Some virus interactions with Nups result in degradation or redistribution of NPC components as happens during poliovirus infection (16-21,25,26). Therefore, we first tested Nup62 protein levels and localization in HSV-infected cells. Protein levels were assayed by Western blotting of extracts from cells that were mock infected or infected with either WT HSV-1 or HSV-1 carrying a deletion of the ICP27 gene (Δ27). During lytic infection with HSV-1 at MOI 10, ICP27 protein starts to

express as early as 2-3 h post infection (hpi) (Fig. 2A, first panel). The levels are readily detectable by 4 h (Fig. 2A, middle panel) and peak between 8-16 h (not shown). GAPDH staining confirmed similar protein loading. As cell lysis begins to occur several hours after ICP27 levels have peaked, ICP27 accumulation was also tested at 24 h at a lower MOI. ICP27 was abundant still at 24 h post-infection, when infected with HSV at an MOI of 1 (Fig. 2A, last panel). No difference in Nup62 protein levels could be observed between mock, WT and ICP27 null virus infected cells at the times tested (Fig. 2A) showing that HSV-1 does not downregulate Nup62 levels.

Next we looked at the effect of HSV-1 infection on Nup62 localization by immunofluorescence. As the aim was to look at the total levels of intact Nup62 in infected cells we chose to analyze Nup62 in directly-fixed cells without triton pre-extraction. Nup62 (green) remains at the nuclear envelope in non-extracted directly-fixed cells, regardless of the presence of ICP27 (red; in 3 and 18 hpi cells) (Fig. 2B). Similar to an earlier report of changes in nuclear pore composition in some uninfected and infected cells (66) we also noted the presence of some microclusters of Nup62 around the nuclear rim at 18 hpi and a distinct speckled cytoplasmic staining in many cells where nuclear integrity was still intact (late HSV-1 infection compromises nuclear integrity) as observed by DAPI staining. Thus, unlike during infection by several other viruses where Nup62 is either degraded or heavily mislocalized, in HSV-infected cells Nup62 protein levels are not much different compared to mock-infected cells but may cluster at the nuclear periphery late in infection.

ICP27 interaction with Nup62 revealed by co-immunoprecipitation — To test for a physical association between ICP27 and Nup62, immunoprecipitation (IP) assays were conducted. Nup62 protein was co-immunoprecipitated with ICP27 Abs only in cells infected with WT virus, but not in cells infected with the ICP27-null virus or mock infected cells (Fig. 3A). The absence of ICP27 protein in the mock and ICP27-null virus immunoprecipitated lysates was confirmed with staining the immunoprecipitated fractions with ICP27 Abs. The presence of Nup62 protein in all the lysates used was confirmed in the unbound panel and the absence of an interaction with control serum Abs (ctr) showed the specificity of the interaction with ICP27 Abs.

In a reverse experiment ICP27 protein was co-immunoprecipitated with Nup62 Abs. In agreement with the above data, no interaction was observed in mock infected and ICP27-null virus infected cell lysates (Fig. 3B). In addition to the interaction observed in WT virus infected cell lysates, an interaction was observed in cell lysates from M16 HSV-1 infected cells. M16 is a mutant virus strain that has a point mutation in the Zn finger motif at the C-terminus of ICP27 (C488L). This mutation has been shown to block interaction with TAP (48). The interaction between ICP27 and Nup62 is not mediated by viral RNA as has been shown for the TAP/NXF1 interaction (48) because interactions were maintained upon treatment of cell extracts with RNase I both during the lysis stage and during immunoprecipitation reactions (Fig. 3B and *Supplementary Fig. S1*). Treatment with RNAse I may provide more sites for specific protein-protein complex formation by reducing the amount of transport receptors bound to RNAs. This could be the reason that more ICP27 co-immunoprecipitated with the anti-Nup62 Ab in the presence of RNAse I. Again, non-specific serum Abs served as a negative control and Nup62 Abs immunoprecipitated Nup62 protein in all lysates (Fig. 3B, lower panels). To address the possibility that another Nup might mediate the interaction between ICP27 and Nup62, several different Abs against different epitopes of Nup62 were employed with the same result (data not shown). Additionally, the possibility that this *in vivo* interaction between ICP27 and Nup62 was specific and does not co-immunoprecipitate irrelevant non-specific proteins was investigated by probing anti-Nup62 co-immunoprecipitations with antibodies to a non-specific protein (*Supplementary Fig. S2*)).

The above reactions were performed using human HeLa cells. To ensure that potential differences in the character of virus infection and cellular proteins do not contribute to the observed ICP27-Nup62 interaction, we also tested for this interaction using hamster BHK cells that are more permissive for HSV-1 infection. A similar interaction between ICP27 and Nup62 was observed in BHK cells (Fig. 3C). Additionally, in this experiment different concentrations of WT infected lysate were used. The relative increase in the ICP27-Nup62 interaction by varying input amounts of lysates with the same antibody concentrations shows that the antibodies were not saturated in these

experiments and supports the specificity of the interaction. As a positive control for ICP27 immunoprecipitation, ICP27 was also immunoprecipitated from WT HSV-1 infected BHK cell lysates with Abs against ICP27 and run on the same gel (Fig. 3C, far right lane).

The ICP27-Nup62 interaction is verified by pull down assay with bacterially purified components — To further confirm the interaction of ICP27 with Nup62 we expressed and purified GST and GST-Nup62 from bacteria and used these proteins to pull down ICP27 from HSV-infected and mock-infected cell extracts. Western blotting with anti-ICP27 Ab showed that GST-Nup62 pulled down ICP27 from WT infected cell extracts (Fig. 4A) but not from ICP27-null infected and mock-infected cell extracts. The ICP27 interaction with Nup62 does not require the presence of other viral proteins as GST-Nup62 could also pull down ICP27 from uninfected HeLa cells expressing ICP27 protein from a transfected plasmid (Fig. 4A, tr27). GST failed to pull down ICP27 from WT HSV-1 infected cell extracts. Bacterially expressed proteins including GST-Nup62 and GST used in these assays are shown in figure 5C. GAPDH Ab confirmed that similar amounts of cell extracts were added to all pull downs (Fig. 4A, lower panel). The interaction with endogenous proteins was RNA-independent as it occurred in RNase I treated extracts (Fig. 4B and *Supplementary Fig. S1*). As a control, another GST fusion protein Rae1 (see below) which is an mRNA export factor involved in nucleocytoplasmic transport was incubated with extracts of cells infected with either WT HSV-1, Δ27 null, a C-terminal ICP27 point mutant (P465L:G466E) HSV-1 strain (M15) or mock infected cell extracts (Fig. 4C). Proteins co-purifying on Glutathione Sepharose beads were analyzed by Western blotting with an Ab against ICP27. Neither GST alone nor GST-Rae1 pulled down ICP27 from any of the cell extracts, which can be seen in the input cell extract lane (upper panel). A doublet band of greater mobility in lanes 2-5 and marked with an asterisk is a band from the GST-Rae1 bacterial protein preparation cross-reacting non-specifically with anti-ICP27 Ab. Input cell extracts and GST alone served as a control for ICP27 in pull downs. GAPDH levels in the lysates served as a loading control for these experiments (lower panel). Bacterially expressed GST-Rae1 protein used in binding assays (Fig. 4C) is shown on a Coomassie stained gel (Fig. 4D).

As a positive control for a Rae1 functional interaction, its ability to bind a known partner protein, Nup98 (67)**,** independent of presence of ICP27, was tested. Bacterially purified GST-Rae1 or GST was incubated in presence of RNase I with extracts of cells infected with Δ27 null mutant HSV-1 strain or mock infected. Proteins co-purifying on Glutathione Sepharose beads were analyzed by Western blotting with an Ab against Nup98. GST-Rae1 pulled down Nup98 from Δ27 infected as well as mock infected cell lysates (Fig. 4E, bound fraction). A similar result was obtained for TAP that interacts with Nup98 (68) using bacterially purified GST-TAP (Fig. 4E, bound fraction). These data demonstrate that in our assay bacterially purified GST-RaeI and GST-TAP were able to bind partner protein Nup98 and RaeI-Nup98 and TAP-Nup98 complexes are formed in the mock as well as virus-infected cells in an RNA-independent manner. Thus, though ICP27 is known to bind TAP receptor, it does not appear to compete with TAP binding to Nup98. GST alone showed a weak band as background in bound samples; however, the majority of Nup98 is not pulled down and is present in unbound samples with GST alone whereas no Nup98 is left as unbound with mock lysates (Fig. 4E).

The Nup62-ICP27 interaction is direct— TAP has previously been shown to bind to ICP27 at both ends (48). Therefore GST-TAP was used as a positive control for proper folding of the bacterially purified tagged ICP27 protein (see below). First, GST-TAP was able to pull down ICP27 from WT HSV-1 infected cell extracts (Fig. 5A upper panel) but not from the ICP27-null virus infected extracts (Δ27) nor from extracts of cells infected with an HSV-1 mutant strain carrying a C-terminal point mutation in ICP27 at the known site of interaction with TAP (M15). As a negative control, GST failed to pull down ICP27 from WT HSV-1 infected cell extracts. TAP interacts with Nup62 (68) so, as a specificity control for the binding reactions shown above, GST-TAP was tested to determine if it was able to interact with Nup62 under the same conditions. Western blot with anti-Nup62 Ab showed that GST-TAP pulled down Nup62 from WT HSV-1 infected cell lysates (Fig. 5A lower panel) as well as from the ICP27-null virus infected lysates and from lysates of cells infected with an HSV-1 virus carrying a C-terminal point mutation in ICP27 (M15) and mock cells. This demonstrates that

TAP-ICP27 (Fig. 5A upper panel) and Nup62-ICP27 complex (Fig. 4 A and B) formed in the WT virus-infected cells whereas the TAP-Nup62 complex formed in both infected (WT, null and M15 mutant) and mock infected cells (Fig. 5A lower panel). To test the RNA requirement for the above binding we performed anti-ICP27 co-immunoprecipitations in the presence of RNase I from various HeLa cell lysates. Western blotting with anti-TAP antibodies showed co-immunoprecipitation of TAP in WT infected HeLa cell lysates in the presence of RNase I by ICP27 but no co-immunoprecipitation with M15, Δ27 and mock infected lysates (Fig. 5B upper panel). Mock infected RNase treated HeLa cell extracts were used as an input positive control for TAP. ICP27 immunoprecipitated itself in WT and M15 infected HeLa cell lysates in the presence of RNase I but no co-immunoprecipitation was observed in Δ27 and mock infected cell lysates (Fig. 5B lower panel).

To test if ICP27 interacts with Nup62 directly, independent of any other bridging factor, His-tagged ICP27 and GST-Nup62 were expressed and purified from *E. coli* for use in an *in vitro* pull down assay. Various proteins used in the *in vitro* binding assays are shown in figure 5C. Western blotting was performed on bound samples using anti-His Ab to identify the bound full-length His-tagged ICP27 protein. Both the purified GST-TAP and GST-Nup62 were able to pull down the purified His-ICP27 in the absence of other viral or mammalian cell proteins (Fig. 5D), confirming that GST-p62 interacts directly *in vitro* with ICP27. The ratio of bound bacterially purified protein compared to the input consistently appeared to be less than the ratio when ICP27 was bound from mammalian cell lysates (Fig. 4A and B) suggesting that some posttranslational modifications may contribute additively to this complex formation. Again, as a negative control GST alone failed to pull down His-ICP27. The bacterially purified proteins in our preparation contain cleavage products of the full-length fusion proteins because it is quite difficult to express and purify non-cleaved full-length proteins from ICP27-family of herpes viral proteins. Although lack of full purification means that there is a possibility that other bacterial proteins in the ICP27 fusion protein preparation mediate any interaction. However, we have included a number of internal negative and positive controls in binding assays that argue against this possibility. Moreover a positive ICP27-Nup62 co-immunoprecipitation occurring with high salt titration (wash with 500mM NaCl) provides additional evidence of specificity of binding (data not shown).

Additionally for the direct *in vitro* pull down assay the specificity was further confirmed using an irrelevant, non-specific His-tagged fusion protein (His-mRFP) expressed in bacteria and purified to the same extent as the IPC27 fusion proteins. The His-mRFP fusion protein, present in all binding reactions, (Fig. 5E, upper panel: band corresponding to the input lane; lower panel: all lanes) did not interact with GST-TAP, GST-Nup62 or GST alone in pull down assays. Hence ICP27 binding to GST-TAP and GST-Nup62 was likely not due to poor protein preparation or other bacterial proteins mediating the binding

The Nup62-ICP27 interaction is conserved across herpesviridae — GST-fusion proteins were also purified for ICP27 and its KSHV homologue ORF57. Both were able to pull down Nup62 from HeLa cell extracts (Fig. 6A). Moreover, the amount of Nup62 associating with GST-ICP27 and GST-ORF57 from the HeLa extracts was very similar (Fig. 6A). No interaction occurred between Nup62 and GST, confirming the specificity of the interaction (Fig. 6A, last lane). The lower band marked with an asterisk in lane 2 is possibly a band from the GST-ICP27 protein preparation cross-reacting non-specifically with Nup62 Abs. To further confirm that non-specific irrelevant proteins did not also bind to ICP27 or ORF57 fusion proteins, pulled down reactions were blotted with anti-GAPDH Ab. This showed GAPDH present only in the input and not in the pulled down samples (Fig. 6B). GST-ICP27, GST-ORF57 and GST alone present on the beads used in the binding reactions are shown in Figure 6C.

Mapping of binding of Nup62 on ICP27 — To map the interacting regions of ICP27 with Nup62 we used purified GST-Nup62 and GST alone to pull down ICP27 from cell lysates infected with WT virus or a panel of ICP27 mutant viruses. The mutants (Fig. 7A) have been previously used for other mapping studies to define the functional domains of ICP27 (37,53-56). In particular, a series of deletion viruses covering the whole N-terminal region was tested including deletions in the NES, NLS, and RGG sequences. Additionally, ICP27 C-terminal point mutant viruses M15 (P465L:G466E) and M16 (C488L) were tested (57); the position of these mutations is shown with double and single

asterisks in the ICP27 cartoon in Figure 7A. GST-Nup62 pulled down all N-terminal ICP27 deletion mutants except for dLeu (aa6-19) that removed the NES (Fig. 7B). Despite significant levels of expression of the ICP27 protein from dLeu mutant virus as seen in unbound lysate fractions (Fig. 7B, lower panels), no ICP27 was pulled down with GST-Nup62. In contrast, other ICP27 N-terminal mutant proteins like those from d1-2 and d3-4 viruses bound to GST-Nup62, as did ICP27 deletions up to d6-7 confirming that apart from the extreme N-terminus most of the N-terminal region is not required. However the N-terminal leucine-rich region may contribute to the interaction of ICP27 with Nup62. Interestingly, neither C-terminal mutant of ICP27 (M15, M16) was pulled down by the GST-Nup62. It is known that expression of ICP27 protein from these C-terminal mutant viruses (M15, M16) is reduced as compared to that of the ICP27 protein from the WT virus (48): we see this also in the unbound lysates (Fig. 7B, lower panels). Nonetheless, the absence of an interaction with viral M15 and M16 C-terminal mutants was not due to our inability to analyze this interaction due to the reduced expression levels of ICP27 mutant protein. When the amount of M15 and M16 input lysates added to the GST-Nup62 pull down reactions was increased the C-terminal mutants still failed to pull down detectable levels of ICP27 (data not shown). Lack of interaction of GST-Nup62 with mock and ICP27-null virus infected lysates (Fig. 7B) and the GST control with WT (far right lane) indicated the specificity of the binding reactions. Thus the C-terminus and a small region of the N-terminal segment appear to be important for ICP27 interactions with Nup62.

ICP27 blocks both M9 and NLS - mediated nucleocytoplasmic transport pathways — The ability of ICP27 to interact directly with a core NPC protein in an RNA-independent manner suggested that ICP27 might have either a more direct role in its own shuttling/recycling or additional as yet undefined effects on other nucleocytoplasmic transport pathways during the course of HSV-1 infection. To test for an effect on other transport pathways ICP27 was expressed together with cargo reporters for different transport pathways. Both reporters had two GFP moieties in tandem to bring them above the free diffusion limit for NPC transport and were able to shuttle. On the N-terminus of both was the HIV Rev NES, which is exported in a CRM1-dependent manner, but this was countered by an M9 signal or strong NLS at the C-terminus. The first reporter, NES-GFP_2-M9 carried the M9 sequence from hnRNP A1 (69) that utilizes transportin as an import receptor and is independent of importin/karyopherin α and β (70). At steady state, this reporter accumulates in the nucleoplasm in HeLa cells (Fig. 8A, middle row central panel), apparently because import is dominant over export. When plasmid (pCMV-ICP27)-encoded ICP27 was co-expressed with the M9 reporter (Fig. 8A, lower right panel), the predominant nuclear localization of the M9 reporter construct was largely abolished (Fig. 8A, middle right panel). Now the reporter was equally distributed between the two compartments, demonstrating an inhibition of the transportin pathway by ICP27. ICP27 is a shuttling protein: at steady state, however, it mostly localizes to the nucleus with some cytoplasmic localization. The amount of ICP27 cytoplasmic localization depends on the cell type, levels of expression, and the time post infection. At late times post infection where there are both elevated levels of ICP27 and of transcribed viral mRNAs, ICP27 localizes also to the cytoplasm, possibly shuttling faster with its substrate mRNAs (47). When ICP27 alone was expressed ectopically from a plasmid (pCMV-ICP27) without the reporter and in the absence of infection, the ICP27 accumulated in both the nucleus and cytoplasm of the cells (Fig. 8A, lower left panel). The partial cytoplasmic localization of ICP27 expressed from plasmid DNA could result from the lack of viral RNA substrates. But also higher expression levels of ICP27 may push some into the cytoplasm. Upon co-expression with reporter cargo receptors, ICP27 localization also appeared to be slightly more cytoplasmic (Fig. 8A, lower right panel) possibly as a result of competition for or, saturation of common factors at nuclear pores. The NES-GFP_2-M9 reporter construct also accumulated in the cytoplasm when co-transfected with another plasmid (pTriEx-ICP27) encoding full-length ICP27 WT protein (Fig. 8B middle panel) further supporting an inhibition of the transportin pathway by ICP27.

To determine if ICP27 inhibition of transport is unique to the transportin-dependent pathway or if ICP27 can inhibit multiple pathways, a second reporter (NES-GFP_2-cNLS) representing the classical importin/karyopherin α/β-dependent import was assayed. This reporter carried the SV40 classical basic NLS. It is able to shuttle because its export out of the nucleus is

mediated by the HIV Rev NES in a CRM1-dependent manner. At steady state, it localized almost exclusively in the nucleus, apparently because its import is dominant over export (Fig. 8C, left middle panel). When ICP27 was co-expressed with the NES-GFP_2-cNLS reporter (Fig. 8C, right panels), the reporter was observed predominantly in the cytoplasm (Fig. 8C, right middle panel) along with ICP27 (Fig. 8C, right lower panel). Thus ICP27 also inhibits the importin/karyopherin transport pathway. Images shown (Fig. 8) are the representative of at least three experiments performed. A similar phenotype of reporter localization distribution also to the cytoplasm was observed in more than 90% of dual co-transfected cells. Very few (<10%) dual transfected cells showed only nuclear localization of the reporters.

To test if this ability of ICP27 to inhibit multiple host cell nucleo-cytoplasmic transport pathways was likely to require its interaction with Nup62, the ICP27 C-terminal mutant M15 that did not interact with Nup62 (Fig. 7B) was expressed from a plasmid independently of viral infection (Fig. 9A and Fig. 9B and C, second panels). The plasmid construct was used because M15 protein levels were lower than WT ICP27 in cells infected with mutant viruses. To determine if this approach increased M15 levels, lysates from cells expressing WT ICP27 or the mutant were analyzed by Western blotting (*Supplementary Fig. S3*). Indeed this yielded similar protein levels for comparison and at similar exposure times, fluorescence intensity of proteins expressed from both was similar too (data not shown). For these experiments both the M9 reporter construct that utilizes transportin as an import receptor (NES-GFP_2-M9) and the cNLS reporter construct that is dependent on the importin/karyopherin α/β pathway (NES-GFP_2-cNLS) were used. Unlike the WT ICP27 that redistributed the reporter to the cytoplasm, the M15 mutant yielded predominantly nuclear staining for the reporters (Figs. 9B and 9C, second panels). This suggests that the interaction of Nup62 with the C-terminal region of ICP27 is required for ICP27 inhibition of host cell transport.

Other ICP27 mutants (Fig. 9A) were also examined for their effects on the NES-GFP_2-M9 (Fig. 9B) or the NES-GFP_2-cNLS (Fig. 9C) reporters using plasmid-encoded ICP27 mutant proteins. Previously in mutant virus infections most of the ICP27 proteins carrying N-terminal deletions were able to interact with Nup62, whereas C-terminal point mutants were not (Fig. 7B). When co-expressed from exogenously introduced plasmids, these ICP27 mutants had variable effects on the localization of the reporter proteins. NES-GFP_2-M9 and NES-GFP_2-cNLS reporters localized also to the cytoplasm in 70 and 80% of cells when co-transfected with the ICP27 N-terminal deletion mutants 10-512 and 166-512 respectively (Fig. 9B and C, middle panels). The N-terminal mutant 10-512, which deletes only part (aa6-9) of ICP27 NES (aa6-19) in 70% of cells showed the phenotype similar to full length WT ICP27 protein (first panels). In some cells (20% cells) nuclear retention of the reporter protein was observed. Whereas for the ICP27 mutant 166-512, altered cytoplasmic redistribution was seen in more cells (80%) compared to nuclear retention (10%). This is in agreement with most of the ICP27 proteins carrying N-terminal deletions able to interact with Nup62 except dleu where NES region alone is missing. Additionally, it indicates existence of alternative routes for shuttling for these N-terminal mutants'. Loss of interaction in dleu may possibly be due to unavailability of interacting sites as a result of altered folding of the mutant protein. Whereas the C-terminal deletion mutant 1-403 and the M15 C-terminal ICP27 point mutant that do not bind to Nup62 did not alter the distribution of the either of the reporters significantly. The staining remained mostly in the nucleus in dual co-expressing cells (Fig. 9B and C, last middle panels). Representative images for are shown in Fig. 9B and C. These results further strengthen the importance of the C-terminal region and ICP27-Nup62 interaction for ICP27 activity.

DISCUSSION

Herpesviruses are nuclear replicating DNA viruses that need to transport mRNAs and proteins across the nuclear envelope because of the compartmentalization of the host cellular transcription and translation machinery upon which the virus depends. Viruses use a variety of mechanisms to selectively block host mRNA export. Understanding the molecular basis of these mechanisms has important implications for developing novel anti-viral treatments. Previous studies on ICP27 interactions with the cellular transport machinery have mostly examined the roles for ICP27-mediated viral RNA export utilizing the cellular mRNA export receptor TAP that allows the intronless herpesvirus mRNAs to

be preferentially transported. To date the mechanism for shuttling of viral RNA-independent free ICP27 has remained inconclusive (47) as ICP27 export is NES region-mediated but not dependent on the receptor CRM1, which is the major NES-recognizing cellular export receptor. Additionally, in virus-infected mammalian cells where ICP27 substrate viral RNAs are also present, ICP27 mRNA export is shown to be TAP dependent using siRNAs to TAP (47-49). However, export of free ICP27 not bound to viral RNA is TAP-independent because constitutive transport element did not inhibit ICP27 export when tested by nuclear microinjection in *Xenopus* oocytes (47). Binding of ICP27 to specific viral RNA substrates could alter either ICP27 conformation or the ICP27/RNA/partner protein complex configuration. The interaction between ICP27 and Nup62 demonstrated here is the first example of herpesviruses able to directly utilize NPC core components and may provide an explanation for discrepancies in attempts to explain ICP27 shuttling. This interaction appears to be functionally relevant as WT ICP27, but not C-terminal mutants that failed to interact with Nup62, can inhibit transport of substrates of some of the cellular transport receptors tested. Such an interaction would provide advantage to the virus as ICP27 may compete with and block transport of host substrates.

TAP- and CRM1-mediated export pathways converge at the NPC as CRM1 competes strongly with TAP for binding to Nup214 and prevents export by the TAP transport domain (71). Competition for binding to a Nup at the nuclear pore is a possible explanation for the inhibition by ICP27 of transport of reporter substrates observed here. As an example of import pathways converging at the NPC, transportin inhibited karyopherin α/β1-mediated import of a classical NLS containing substrate and, *vice versa*, karyopherin β1 inhibited transportin-mediated import of the hnRNP A1-based substrate, suggesting that the two import pathways merge at the level of docking of β1 and transportin to Nups (8,9). Thus ICP27 may shuttle by utilizing different components of the host transport machinery, possibly varying pathways at different stages of the viral replication cycle.

Several cellular and viral proteins continuously shuttle between nuclear and cytoplasmic compartments, including heterogeneous nuclear RNP (hnRNP) proteins (72,73), U1 small nuclear RNP-specific protein U1A (74) and influenza virus NS1 (75) and HIV-1 Rev protein (76). Although the physiological significance of nuclear shuttling is not known in all cases, some RNA-binding shuttling proteins have roles in mRNA export. hnRNP A1 associates with RNA polymerase II-derived-transcripts in both the nucleus and cytoplasm and is thought to directly mediate their transport (73). ICP27 is able to efficiently shuttle in the presence of CRM1 inhibitor LMB, as addition of LMB did not inhibit the export of ICP27 (77). These recent data and several earlier reports (47-49) show that ICP27 does not require CRM1 for its nuclear export. ICP27 interacts with Aly/REF, which recruits the TAP cellular mRNA export pathway (47,49) and TAP/NXF1 is required for export (48). However, recent data show that Aly/REF is dispensable for ICP27-mediated export of HSV mRNA (78). Moreover, Aly/REF knockdown has little effect on viral RNA export (42). HIV-1 Rev protein binds to Rev-response elements in viral mRNAs to mediate their export and also interacts with core Nups via CRM1 (79). HSV-1 ICP27 is known to bind intronless RNAs and function in their export (reviewed in 28,29) and we postulate that, like HIV Rev, ICP27 could use core Nups in this transport process.

Using a heterokaryon assay able to test the shuttling activity of proteins, ICP27 WT was able to shuttle efficiently (80). Shuttling of some of the ICP27 mutants has also been tested. Mutant d1-2 (which deletes aa12-63, including part of NES: aa 6-19) showed reduced shuttling (80). The ICP27 M15 C-terminal point mutant completely abrogates shuttling activity (80**.** M15 virus is totally replication defective (57). Whereas, deletion of ICP27 NES (aa 6-19) in the dleu mutant weakened but did not abrogate shuttling and dleu is replication deficient (77).

That mutations in amino acids 6-11 at the N-terminus and mutations at the C-terminus of ICP27 both affect the interaction *in vitro* with bacterially purified Nup62 suggests that both regions of ICP27 may act together for Nup62 binding. However, N-terminal mutant 10-512, which deletes part (aa 6-9) of ICP27 NES (aa 6-19) when used in the transport assay, in 70% of cells showed the phenotype similar to full length WT protein. In fewer cells nuclear retention of the reporter protein was also observed. Our observations are similar to the ones reported earlier that mutant d1-2 (which deletes aa12-63, including part of NES-aa 6-19) showed reduced shuttling (80) and in the dleu mutant deletion of

NES (aa 6-19) of ICP27 weakened but did not abrogate shuttling. Mutant ICP27 dleu virus is replication deficient (77) but not replication defective. Hence, for these N-terminal mutants' alternative routes for nuclear egress appear to exist when other regions of the protein especially the C-terminus are intact. Our observations are not quantitative in nature but help to understand the role(s) played by various segments of ICP27. From the ICP27-Nup62 interaction even in the presence of LMB (*Supplementary Fig. S2*) and from transport assays utilizing various N- and C-terminal ICP27 plasmid mutations, it becomes clear that though the N-terminal region of ICP27 affects its ability to bind Nup62 *in vitro*, functionally it appears to be the C-terminus of ICP27 that acts as the major region of importance for shuttling of viral protein. These data revealed that mutants that reduce protein-protein interactions with Nup62 at the C-terminus alter and dramatically decrease the ability of ICP27 to shuttle and also inhibit multiple host cell nucleo-cytoplasmic transport pathways. The ICP27 M15 mutant protein appears to be able to enter the nucleus after synthesis in the cytoplasm via alternative routes; however, its ability to export out of nucleus seems to be defective. Loss of Nup62 interaction correlates with the inability of M15 to re-export and shuttle continuously and it appears that as a result of loss of this crucial function M15 is replication defective (57). With regards to cellular and viral mRNA processing, HeLa cells infected with M15 mutant virus failed to accumulate cellular unspliced α–globin pre-mRNA and mutation in the M15 virus greatly increase the length and heterogeneity of the poly(A) tail of spliced α–globin mRNA (81). Additionally, ICP0 is one of the few intron-containing viral genes and it yielded no detectable intron 1-containing transcripts in M15 infections (81). M15 protein has been reported to have an exclusively nuclear distribution (80) and in contrast to the WT ICP27 protein, the M15 mutant protein was absent from the polyribosome fractions (40). It remains possible however, that the M15 mutation might affect other activities of ICP27 than NPC interaction.

Involvement of the CRM1-independent, extreme N-terminus leucine-rich NES region of ICP27 in its interaction with Nup62 may simply be due to a structural requirement of ICP27 in forming a viable conformation *in vivo*. Recent data indicates that ICP27 can acquire an intramolecular head-to-tail conformation (45) that could provide such a binding site involving both ends of the ICP27 molecule. The intramolecular head-to-tail configuration prevents the interaction of ICP27 with RNA pol II (45). It is tempting to speculate that certain post-translational modifications of ICP27 during infection, such as its phosphorylation and arginine methylation (58,82), could direct such changes in conformation. This conformational alteration may promote specificity and/or preference for certain partner proteins such as Nup62 or TAP, especially as both of these modifications are important for ICP27 export, viral replication and gene expression functions (83,84). ICP27 also multimerizes via its C-terminus, which could generate large complexes resulting in increased binding sites available for Nup62 and/or transport receptors. The study of the relationship between ICP27 structural conformations and regulation of binding partners will be an important area for future work.

RNA viruses that replicate exclusively in the cytoplasm block host transport completely e.g. by active degradation of Nup62 and Nup153 in poliovirus and rhinovirus-infected cells. In contrast, ICP27 appears to dominantly utilize the host transport machinery in support of export of intronless viral mRNAs and import of viral regulatory and capsid and tegument proteins for assembly in the nucleoplasm. Consistent with this and an earlier study of NPC component localization during herpes virus infection (66) we found Nup62 protein intact and properly localized in HSV-1 infected cells and an ICP27 mutant deficient for Nup62 binding failed to inhibit cellular nucleocytoplasmic transport pathways. It will be interesting in future to test for ICP27 interactions with other Nups.

SUPPLEMENTAL MATERIALS

Three Supplemental Figures (*Figs. S1, S2 and S3*).

REFERENCES

1. Pasdeloup, D., Blondel, D., Isidro, A. L., and Rixon, F. J. (2009) *J Virol* **83**, 6610-6623
2. Copeland, A. M., Newcomb, W. W., and Brown, J. C. (2009) *J Virol* **83**, 1660-1668
3. Pellet, P. E., and Roizman, B. (2007) The Herpesviridae Family: A Brief Introduction. in *Fields' Virology* (Knipe, D. M., and Howley, P. M. eds.), 5th Ed., Wolters Kluwer Health/Lippincott Williams & Wilkins, Philadelphia. pp
4. Wente, S. R. (2000) *Science* **288**, 1374-1377
5. Strambio-De-Castillia, C., Niepel, M., and Rout, M. P. (2010) *Nat Rev Mol Cell Biol* **11**, 490-501
6. Wagstaff, K. M., and Jans, D. A. (2009) *Traffic* **10**, 1188-1198
7. Arnold, M., Nath, A., Hauber, J., and Kehlenbach, R. H. (2006) *J Biol Chem* **281**, 20883-20890
8. Bonifaci, N., Moroianu, J., Radu, A., and Blobel, G. (1997) *Proc Natl Acad Sci U S A* **94**, 5055-5060
9. Fridell, R. A., Truant, R., Thorne, L., Benson, R. E., and Cullen, B. R. (1997) *J Cell Sci* **110 (Pt 11)**, 1325-1331
10. Fornerod, M., Ohno, M., Yoshida, M., and Mattaj, I. W. (1997) *Cell* **90**, 1051-1060
11. Fischer, U., Huber, J., Boelens, W. C., Mattaj, I. W., and Luhrmann, R. (1995) *Cell* **82**, 475-483
12. Pasquinelli, A. E., Ernst, R. K., Lund, E., Grimm, C., Zapp, M. L., Rekosh, D., Hammarskjold, M. L., and Dahlberg, J. E. (1997) *EMBO J* **16**, 7500-7510
13. Saavedra, C., Felber, B., and Izaurralde, E. (1997) *Curr Biol* **7**, 619-628
14. Strasser, K., and Hurt, E. (2000) *EMBO J* **19**, 410-420
15. Gruter, P., Tabernero, C., von Kobbe, C., Schmitt, C., Saavedra, C., Bachi, A., Wilm, M., Felber, B. K., and Izaurralde, E. (1998) *Mol Cell* **1**, 649-659
16. Petersen, J. M., Her, L. S., and Dahlberg, J. E. (2001) *Proc Natl Acad Sci U S A* **98**, 8590-8595
17. Gustin, K. E., and Sarnow, P. (2001) *EMBO J* **20**, 240-249
18. Gustin, K. E., and Sarnow, P. (2002) *J Virol* **76**, 8787-8796
19. Nelson, L. M., Rose, R. C., and Moroianu, J. (2003) *Virology* **306**, 162-169
20. Darshan, M. S., Lucchi, J., Harding, E., and Moroianu, J. (2004) *J Virol* **78**, 12179-12188
21. Park, N., Skern, T., and Gustin, K. E. (2010) *J Biol Chem* **285**, 28796-28805
22. Faria, P. A., Chakraborty, P., Levay, A., Barber, G. N., Ezelle, H. J., Enninga, J., Arana, C., van Deursen, J., and Fontoura, B. M. (2005) *Mol Cell* **17**, 93-102
23. Satterly, N., Tsai, P. L., van Deursen, J., Nussenzveig, D. R., Wang, Y., Faria, P. A., Levay, A., Levy, D. E., and Fontoura, B. M. (2007) *Proc Natl Acad Sci U S A* **104**, 1853-1858
24. Macaulay, C., Meier, E., and Forbes, D. J. (1995) *J Biol Chem* **270**, 254-262
25. Fontoura, B. M., Faria, P. A., and Nussenzveig, D. R. (2005) *IUBMB Life* **57**, 65-72
26. Gustin, K. E. (2003) *Virus Res* **95**, 35-44
27. Tsuji, T., Sheehy, N., Gautier, V. W., Hayakawa, H., Sawa, H., and Hall, W. W. (2007) *J Biol Chem* **282**, 13875-13883
28. Sandri-Goldin, R. M. (2008) *Front Biosci* **13**, 5241-5256
29. Smith, R. W. P., Malik, P., and Clements, J. B. (2005) *Biochem Soc Trans* **33**, 499-501
30. Malik, P., Blackbourn, D. J., and Clements, J. B. (2004) *J Biol Chem* **279**, 33001-33011
31. Hiriart, E., Farjot, G., Gruffat, H., Nguyen, M. V., Sergeant, A., and Manet, E. (2003) *J Biol Chem* **278**, 335-342
32. Han, Z., and Swaminathan, S. (2006) *J Virol* **80**, 5251-5260
33. Gruffat, H., Batisse, J., Pich, D., Neuhierl, B., Manet, E., Hammerschmidt, W., and Sergeant, A. (2002) *J Virol* **76**, 9635-9644
34. Rice, S. A., and Knipe, D. M. (1988) *J Virol* **62**, 3814-3823
35. Sekulovich, R. E., Leary, K., and Sandri-Goldin, R. M. (1988) *J Virol* **62**, 4510-4522
36. McCarthy, A. M., McMahan, L., and Schaffer, P. A. (1989) *J Virol* **63**, 18-27
37. Rice, S. A., and Knipe, D. M. (1990) *J Virol* **64**, 1704-1715
38. Hardwicke, M. A., and Sandri-Goldin, R. M. (1994) *J Virol* **68**, 4797-4810
39. Fontaine-Rodriguez, E. C., and Knipe, D. M. (2008) *J Virol* **82**, 3538-3545

40. Larralde, O., Smith, R. W. P., Wilkie, G. S., Malik, P., Gray, N. K., and Clements, J. B. (2006) *J Virol* **80**, 1588-1591
41. Ellison, K. S., Maranchuk, R. A., Mottet, K. L., and Smiley, J. R. (2005) *J Virol* **79**, 4120-4131
42. Escudero-Paunetto, L., Li, L., Hernandez, F. P., and Sandri-Goldin, R. M. *Virology* **401**, 155-164
43. Long, J. C., and Caceres, J. F. (2009) *Biochem J* **417**, 15-27
44. Pearson, A., Knipe, D. M., and Coen, D. M. (2004) *J Virol* **78**, 23-32
45. Hernandez, F. P., and Sandri-Goldin, R. M. (2010) *J Virol* **84**, 4124-4135
46. Zhi, Y., Sciabica, K. S., and Sandri-Goldin, R. M. (1999) *Virology* **257**, 341-351
47. Koffa, M. D., Clements, J. B., Izaurralde, E., Wadd, S., Wilson, S. A., Mattaj, I. W., and Kuersten, S. (2001) *EMBO J* **20**, 5769-5778
48. Chen, I. H., Li, L., Silva, L., and Sandri-Goldin, R. M. (2005) *J Virol* **79**, 3949-3961
49. Chen, I. H., Sciabica, K. S., and Sandri-Goldin, R. M. (2002) *J Virol* **76**, 12877-12889
50. Soliman, T. M., and Silverstein, S. J. (2000) *J Virol* **74**, 2814-2825
51. Lilley, C. E., Groutsi, F., Han, Z., Palmer, J. A., Anderson, P. N., Latchman, D. S., and Coffin, R. S. (2001) *J Virol* **75**, 4343-4356
52. Soliman, T. M., and Silverstein, S. J. (2000) *J Virol* **74**, 7600-7609
53. Lengyel, J., Guy, C., Leong, V., Borge, S., and Rice, S. A. (2002) *J Virol* **76**, 11866-11879
54. Rice, S. A., Lam, V., and Knipe, D. M. (1993) *J Virol* **67**, 1778-1787
55. Aubert, M., Rice, S. A., and Blaho, J. A. (2001) *J Virol* **75**, 1013-1030
56. Mears, W. E., Lam, V., and Rice, S. A. (1995) *J Virol* **69**, 935-947
57. Rice, S. A., and Lam, V. (1994) *J Virol* **68**, 823-833
58. Mears, W. E., and Rice, S. A. (1996) *J Virol* **70**, 7445-7453
59. Braun, I. C., Rohrbach, E., Schmitt, C., and Izaurralde, E. (1999) *EMBO J* **18**, 1953-1965
60. Bryant, H. E., Matthews, D. A., Wadd, S., Scott, J. E., Kean, J., Graham, S., Russell, W. C., and Clements, J. B. (2000) *J Virol* **74**, 11322-11328
61. Hutten, S., Flotho, A., Melchior, F., and Kehlenbach, R. H. (2008) *Mol Biol Cell* **19**, 2300-2310
62. Siomi, H., and Dreyfuss, G. (1995) *J Cell Biol* **129**, 551-560
63. Phelan, A., Carmo-Fonseca, M., McLaughlan, J., Lamond, A. I., and Clements, J. B. (1993) *Proc Natl Acad Sci U S A* **90**, 9056-9060
64. Gerace, L., Ottaviano, Y., and Kondor-Koch, C. (1982) *J Cell Biol* **95**, 826-837
65. Malik, P., Korfali, N., Srsen, V., Lazou, V., Batrakou, D. G., Zuleger, N., Kavanagh, D. M., Wilkie, G. S., Goldberg, M. W., and Schirmer, E. C. (2010) *Cell Mol Life Sci* **67**, 1353-1369
66. Hofemeister, H., and O'Hare, P. (2008) *J Virol* **82**, 8392-8399
67. Pritchard, C. E., Fornerod, M., Kasper, L. H., and van Deursen, J. M. (1999) *J Cell Biol* **145**, 237-254
68. Bachi, A., Braun, I. C., Rodrigues, J. P., Pante, N., Ribbeck, K., von Kobbe, C., Kutay, U., Wilm, M., Gorlich, D., Carmo-Fonseca, M., and Izaurralde, E. (2000) *RNA* **6**, 136-158
69. Michael, W. M., Choi, M., and Dreyfuss, G. (1995) *Cell* **83**, 415-422
70. Pollard, V. W., Michael, W. M., Nakielny, S., Siomi, M. C., Wang, F., and Dreyfuss, G. (1996) *Cell* **86**, 985-994
71. Schmitt, I., and Gerace, L. (2001) *J Biol Chem* **276**, 42355-42363
72. Flach, J., Bossie, M., Vogel, J., Corbett, A., Jinks, T., Willins, D. A., and Silver, P. A. (1994) *Mol Cell Biol* **14**, 8399-8407
73. Pinol-Roma, S., and Dreyfuss, G. (1992) *Nature* **355**, 730-732
74. Kambach, C., and Mattaj, I. W. (1992) *J Cell Biol* **118**, 11-21
75. Li, Y., Yamakita, Y., and Krug, R. M. (1998) *Proc Natl Acad Sci U S A* **95**, 4864-4869
76. Meyer, B. E., and Malim, M. H. (1994) *Genes Dev* **8**, 1538-1547
77. Lengyel, J., Strain, A. K., Perkins, K. D., and Rice, S. A. (2006) *Virology* **352**, 368-379
78. Johnson, L. A., Li, L., and Sandri-Goldin, R. M. (2009) *J Virol* **83**, 6335-6346
79. Cullen, B. R. (1994) *Infect Agents Dis* **3**, 68-76
80. Mears, W. E., and Rice, S. A. (1998) *Virology* **242**, 128-137
81. Ellison, K. S., Rice, S. A., Verity, R., and Smiley, J. R. (2000) *J Virol* **74**, 7307-7319
82. Zhi, Y., and Sandri-Goldin, R. M. (1999) *J Virol* **73**, 3246-3257
83. Rojas, S., Corbin-Lickfett, K. A., Escudero-Paunetto, L., and Sandri-Goldin, R. M. (2010) *J Virol* **84**, 2200-2211
84. Souki, S. K., Gershon, P. D., and Sandri-Goldin, R. M. (2009) *J Virol* **83**, 5309-5320

ACKNOWLEDGEMENTS

This article is dedicated to the memory of late Prof J. Barklie Clements (JBC). His-ICP27 plasmid and His-mRFP protein were kind gifts from Prof J. B. Clements and Dzmitry G. Batrakou respectively. This work was supported by a Royal Society UK Research Grant to PM (RG090330) and an MRC programme grant (G9826324 to JBC/SVG). PM is recipient of a Royal Society Research Fellowship Award (DH051766). AJ was funded by a PhD studentship from the Education section of Ministry of Health and Medical Sciences, Iran. RI was funded by a Royal Society Undergraduate Summer Studentship awarded to PM (SS072172). ECS and NK are supported by Wellcome Trust Senior Research Fellowship 076616. The Wellcome Trust Centre for Cell Biology is supported by core funding from the Wellcome Trust 077707.

[2] The **abbreviations** used are: **NPC,** nuclear pore complex; **Nups,** nucleoporins; **NLS,** nuclear localization signal; **NES,** nuclear export signal; **HIV**, human immunodeficiency virus; **SV40,** simian virus 40; **HSV-1,** herpes simplex virus type 1; **KSHV,** Kaposi's Sarcoma-associated herpes virus; **EBV,** Epstein-Barr virus; **WT,** wild-type; **MOI,** multiplicity of infection; **PAGE,** SDS- polyacrylamide gel electrophoresis; **GST,** glutathione *S*-transferase; **hpi,** hours post infection.

Key words: Herpes simplex virus type 1 (HSV-1), ICP27, KSHV, ORF57, nucleoporin Nup62, nuclear pore complex (NPC), protein interaction, nucleocytoplasmic transport, import export.

FIGURE LEGENDS

FIGURE 1. **ICP27 associates at the nuclear periphery.** HeLa cells infected with HSV-1 vBSGFP27 (encoding wild-type [WT] ICP27 fused to GFP) were extracted with 1% Triton X-100 prior to fixation at the post-infection times indicated. This treatment removes protein that is not bound to resistant structures such as the nuclear envelope lamina, NPCs, and chromatin. *A,* After fixation the extracted cells were stained for mab414 that recognizes several nucleoporins based on their unique O-linked glycosylation. The extraction removed enough of the diffuse nucleoplasmic pool of ICP27-GFP to be able to observe an ICP27 rim at the nuclear envelope that co-localizes with the NPC. Arrows point to the outer limit of the ICP27-GFP and the NPC staining. No co-localization was observed at the 4 h post-infection time point. In contrast at 8 and 16 h post-transfection significant co-localization can be observed. One region of the 16 h post-infection time point is enlarged in the lower panels. *B,* The same experiment as in *A* was performed except that the transport receptor TAP, which has previously been shown to interact with ICP27, was stained for instead of the nucleoporins. Here small, boxed sections are enlarged in some panels to more clearly observe the co-localization between ICP27 and TAP and two panels for each time point are shown. All images are deconvolved from stacks with individual sections shown and scale bars for both *A* and *B* are 10 μm.

FIGURE 2. **Nup62 integrity during HSV-1 infection.** *A,* Nup62 protein is stable in HSV-1 infected cells. Lysates were prepared from mock infected HeLa cells or HeLa cells infected with WT HSV-1 17+ or an HSV-1 mutant with a deletion of the ICP27 gene (Δ27). Cell lysates shown were prepared at 2, 4, and 24 h post-infection. MOIs used here are 10 for 2 and 4 h time points and 1 for 24 h. Each lysate was reacted on Western blots with Abs to ICP27, Nup62, and GAPDH as a loading control. No obvious differences were observed in Nup62 protein levels at any of the time points. *B,* Nup62 localization is also similar in HSV-1 infected cells. HeLa cells either mock or WT HSV-1 vBSGFP27-infected were fixed directly at 3 hpi and 18 hpi and then permeabilized and stained with Nup62 Abs. Viral ICP27 expression from its endogenous promoter tagged with GFP confirmed that individual cells were infected with HSV-1. The distribution of Nup62 remained mostly peripheral in mock and virus infected cells at early time points (3 hpi). At 18 hpi some distinct cytoplasmic speckles of Nup62 were also seen although nuclear rim localization of Nup62 was still maintained. The vBSGFP27 virus used here has a slightly slower growth rate compared to WT HSV-1 (52). Arrows point to regions with particular clustering of Nup62.

FIGURE 3. **Co-immunoprecipitation of ICP27 and Nup62.** *A,* ICP27 Abs co-immunoprecipitate Nup62. Left panels, Abs against ICP27 were incubated with extracts from mock infected, WT HSV-1 infected, and Δ27 infected HeLa cell lysates. Immunoprecipitated complexes were analyzed by Western blotting with Abs against Nup62. Nup62 co-immunoprecipitated with ICP27 from WT HSV-1 infected HeLa cell extracts, but not from mock or Δ27-infected cell extracts. Reaction of blots with Abs against ICP27 confirms that ICP27 was only expressed in WT HSV-1 infected cells. Western blots of the unbound material in reactions confirmed that Nup62 was present in all reactions. A non-specific mouse serum Ab was used as a negative control (ctr) that failed to co-immunoprecipitate either ICP27 or Nup62 in WT HSV-1 infected lysates. The band marked with an asterisk is the heavy chain of IgGs used for immunoprecipitations. *B,* The reverse immunoprecipitation reaction also indicates an ICP27-Nup62 interaction. Nup62 Ab (H-122) co-immunoprecipitated ICP27 from extracts of HeLa cells infected with either WT or a mutant HSV-1 strain (M16) carrying a C-terminal point mutant (C488L) in ICP27. As expected no band corresponding to the molecular weight of ICP27 was observed co-precipitating with Nup62 Abs from mock Δ27 virus infected cell lysates. Again a non-specific control serum Ab (ctr) failed to co-immunoprecipitate either Nup62 or ICP27 and Nup62 was immunoprecipitated from all lysates with the Nup62 Abs. The band marked with an asterisk is the heavy chain of IgGs used for immunoprecipitations. *C,* The interaction between HSV-1 ICP27 and the host organism Nup62 is conserved across species as Nup62 Ab C-16 co-immunoprecipitated ICP27 from HSV-1-infected BHK cell extracts also. 100 µg of lysate was used for the WT in lane 2 while only 50 µg was used for the WT in lane 4. Again the control Ab failed to co-precipitate ICP27 from WT infected cell extracts. As a positive control for the experiment ICP27 was immunoprecipitated using Abs against ICP27 from WT HSV-infected cells and run on the same gel and blotted with anti-ICP27 Ab.

FIGURE 4. **Interaction of GST-Nup62 and ICP27 does not depend on RNA or virus infection.** *A,* Nup62 fused to glutathione S-transferase (GST) and purified from bacteria in absence of any other mammalian proteins. Nup62-GST was incubated with WT HSV-1, Δ27, and mock-infected cell extracts or with extracts from uninfected cells expressing ICP27 from a plasmid behind the CMV promoter. Upper panel, Western blotting with Abs against ICP27. Lower panel, Western blotting with GAPDH Abs as a loading control for lysates. Input and pulldowns with GST alone were added on the ends for controls. *B,* GST-Nup62 was incubated with WT HSV-1 infected lysates either with or without RNase I treatment. Again GST alone and input are used as controls. *C*, Rae1, another transport receptor does not pull down ICP27. Bacterially purified GST-Rae1 (67 kDa) was incubated with lysates from WT HSV-1, Δ27 null virus, a mutant HSV-1 strain (M15) carrying a C-terminal point mutant (P465L:G466E) in ICP27, or mock infected cells. Upper panel, Proteins co-purifying on Glutathione Sepharose beads were analyzed by Western blotting with Ab against ICP27. GST-Rae1 did not pull down ICP27 from any of the added cell extracts. A doublet band running lower in lanes 2-5 and marked with an asterisk is a band from GST-Rae1 bacterial protein preparation cross-reacting non-specifically with anti-ICP27 Ab. *D*, Bacterially expressed GST-Rae1 protein from the fusion protein preparation used in binding assays shown in figure 4C was analyzed on a coomassie stained gel. Expected full-length protein position is shown with an asterisk while the double asterisks indicates cleavage products of the full-length protein. E, GST-Rae1 and GST-TAP pull down known partner protein Nup98. Bacterially purified fusion protein GST-Rae1 (67kDa) was incubated in presence of RNase I with HSV-1 Δ27 null virus-infected or mock infected cell lysates. Another fusion protein GST-TAP earlier shown to interact with Nup98 and GST alone were also incubated with HSV-1 WT virus-infected cell lysates. Proteins co-purifying on Glutathione Sepharose beads shown as bound samples and unbound leftover samples were analyzed by Western blotting with Ab against Nup98. Mock infected and Δ27 null virus-infected cell lysates were loaded as input. Bound samples show that GST-Rae1 pulled down Nup98 from Δ27 null virus-infected or mock-infected cell lysates and GST-TAP also pulled down Nup98 from WT virus-infected lysates. GST alone showed a weak band as background in bound samples, however the majority of Nup98 is not pulled down and is present in unbound samples with GST alone whereas not much is left as unbound with mock.

FIGURE 5. **The Nup62-ICP27 interaction is direct and TAP also binds ICP27 under similar conditions.** *A,* GST-TAP pulls down ICP27 from WT HSV-1 infected cell extracts, but not from extracts of cells infected with a viral ICP27 C-terminal point mutant (M15; upper panel) whereas in the same binding reactions GST-TAP pulls down Nup62 from WT HSV-1 infected cell extracts, from extracts of cells infected with a viral ICP27 C-terminal point mutant (M15), with ICP27-null mutant Δ27 virus, and from mock-infected cell extracts (upper panel). Bacterially expressed GST or GST-TAP was incubated with extracts from WT, Δ27, or M15 infected HSV-1 strains. Proteins co-purifying on Glutathione Sepharose beads were analyzed by Western blot with ICP27 or Nup62 Abs. *B,* ICP27 and TAP co-immunoprecipitate from HeLa

cell extracts in the presence of RNase I. Co-immunoprecipitation was carried out by mixing anti-ICP27 antibodies 1113 and 1119 with HSV-1 WT and ICP27 mutant M15 and null Δ27 viruses and mock infected HeLa cell extracts. Complexes formed were separated by SDS-PAGE followed by western blotting with anti-TAP and ICP27 Abs. ICP27 co-precipitated TAP; Upper panel shows co-immunoprecipitation of TAP in WT infected HeLa cell extracts in the presence of RNase I by ICP27 but no co-immunoprecipitation with M15, Δ27 and mock infected. Input, mock infected HeLa cell extract. The lower band in the input lane could be due to another cellular protein cross-reacting with this TAP Ab, but the correct size upper band specific to TAP is clearly seen. The band marked with an asterisk is the heavy chain of IgGs used for immunoprecipitations. ICP27 immunoprecipitated itself: Lower panel shows immunoprecipitation of ICP27 in WT and M15 infected HeLa cell extracts in the presence of RNase I by its Ab but no immunoprecipitation in Δ27 and mock infected cell extracts. *C,* The purity of various fusion proteins used for *in vitro* binding assays. Coomassie stained 10% SDS-PAGE of bacterially expressed proteins used in figures 4-7. Single asterisk indicates the molecular weight of the expected protein product while the double asterisks indicates cleavage products of the full-length protein. Pre-stained molecular weight protein markers are loaded on the leftmost lane with GST alone. *D,* Bacterially purified His-tagged ICP27 was incubated with bacterially purified GST-Nup62, GST, or GST-TAP proteins on Glutathione Sepharose beads. Protein complexes formed were eluted by reduced glutathione and separated by SDS-PAGE and Western blotted with anti-His Ab. His-ICP27 interacted with GST-Nup62 and GST-TAP, but not GST alone. *E,* An unrelated non-specific His-tagged fusion protein (His-mRFP) does not interact with GST-tagged TAP or Nup62 fusion proteins. Bacterially purified His-tagged mRFP fusion protein was incubated with bacterially purified GST-TAP, GST-Nup62 or GST alone on Glutathione Sepharose beads in the presence of RNase I. Protein complexes eluted by reduced glutathione and separated by SDS-PAGE are shown on a coomassie stained gel. His-mRFP (corresponding to the band in input) does not interact with GST-TAP, GST-Nup62 and GST alone in bound samples run on gel (upper panel) but His-mRFP is present in all unbound pull down samples run on coomassie (lower panel). Purified His-mRFP alone protein added to the pull down reactions was loaded as input. Molecular weight protein marker sizes are given in kDa on the left.

FIGURE 6. **Nup62 interacts with ORF57, an ICP27 homologue from KSHV.** *A,* Mock-infected HeLa extracts were incubated with either GST-ICP27, GST-ORF57 — a homologue of ICP27 from Kaposi's sarcoma-associated herpesvirus (KSHV), or GST alone. Complexes isolated on Glutathione Sepharose beads were eluted after washing, separated on 10% SDS-PAGE, transferred to nitrocellulose membranes and incubated with Abs against Nup62. Both ICP27 homologs pulled down Nup62. 33% of the HeLa cell extracts used for binding was loaded as input and 1/2 of the pull down reaction samples eluted from the beads was loaded on the gel. Lower band marked with asterisk in lane 2 is a band from GST-ICP27 protein preparation cross-reacting non-specifically with Nup62 Ab. *B,* Control protein GAPDH did not bind to ICP27 and ORF57 fusion proteins. Pulled down reactions of ICP27, ORF57 fusion proteins and GST alone with HeLa lysates were blotted with anti-GAPDH Ab and this showed GAPDH present only in the input and not pulled down in bound samples. *C,* Coomassie stained 10% SDS-PAGE of bacterially expressed proteins GST-ICP27, GST-ORF57 and GST alone present on the beads used in the binding reactions here and in figure 5A. Single asterisk indicates the molecular weight of the expected protein product while the double asterisks indicate cleavage products of the full-length protein.

FIGURE 7. **Mapping of Nup62 interaction sites on ICP27.** *A,* Schematic of ICP27, N-terminal deletion mutants, and C-terminal point mutants. The NES, NLS, and the RGG viral RNA binding site are marked along with the three hnRNP K homology domains (KH1-3). In the third conserved domain are the Sm and Zn finger regions that are respectively disrupted by the M15 (P465L:G466E) and M16 point mutations (C488L) (57) and are respectively represented with double and single asterisks. *B*, GST-Nup62 was incubated with lysates from cells infected with herpesviruses carrying the listed ICP27 mutations. The material that bound to GST-Nup62 and eluted from Glutathione Sepharose beads is shown in the upper panels while the unbound is shown in the lower panels to confirm that the viral proteins were expressed. All co-precipitated proteins are visualized with the ICP27 monoclonal Abs; either 1113 or 1119 as 1113 Ab is raised against a region of ICP27 that is missing in mutant d3-4 and 1119 Ab is raised against a region that is missing in dleu mutant. Standard GST alone and input controls were employed.

FIGURE 8. **ICP27 blocks both NLS and M9-mediated nucleocytoplasmic transport pathways.** *A,* Left panels, ICP27 accumulates both in the nucleoplasm and the cytoplasm of uninfected cells transfected with a WT ICP27-encoding plasmid. Middle panels, HeLa cells were transfected with a plasmid encoding just a NES-GFP_2-M9 reporter that contains the CRM1-dependent NES of HIV-1 Rev and the transportin-dependent M9-NLS of hnRNPA1. This construct accumulates in the nucleoplasm when transfected alone,

but in the cytoplasm when co-transfected with ICP27 (right panels). *B,* NES-GFP_2-M9 reporter construct when co-transfected with ICP27 encoded from pTriEx-ICP27 WT plasmid also accumulates predominantly in the cytoplasm. *C,* Similarly, a different reporter was used (NES-GFP_2-cNLS) that contains the CRM1-dependent REV NES and the importin/karyopherin α/β-dependent (classical) NLS. It accumulates in the nucleoplasm when expressed alone (left panels) and in the cytoplasm when both ICP27 and NES-GFP_2-cNLS are co-transfected (right panels). Scale Bar, 10 μM.

FIGURE 9. **Effect of ICP27 mutants on both NLS and M9-mediated nucleocytoplasmic transport pathways.** *A,* Schematic of mRFP-M15 ICP27 point mutant fusion protein, N-terminal, and C-terminal deletion mutants. Sm region is disrupted by the M15 (P465L:G466E) point mutations (57) with the position of the mutation shown with double asterisks. N-terminal (aa10-512, 166-512) and C-terminal (aa1-403) deletion mutants are expressed from pTriEx-1.1 vector. *B*, The NES-GFP_2-M9 reporter construct accumulates in both the cytoplasm and nucleoplasm when co-transfected with a plasmid encoding WT ICP27 fused to mRFP (mRFP-ICP27 WT) or several N-terminal deletion mutants (pTriEx-ICP27 aa10-512, 166-512), but with the M15 ICP27 C-terminal point mutant and the C-terminal deletion mutant (pTriEx-ICP27 aa1-403), the reporter accumulated in the nucleoplasm indicating that an intact functional C-terminus is required. *C,* The NES-GFP_2-cNLS reporter construct accumulated in the cytoplasm when co-transfected with ICP27 encoded from mRFP-ICP27 WT and N-terminal deletion mutants, but when cells were instead co-transfected with the M15 ICP27 point mutant or the C-terminal (aa1-403) deletion mutant the reporter accumulated in the nucleoplasm.

FIGURE 1

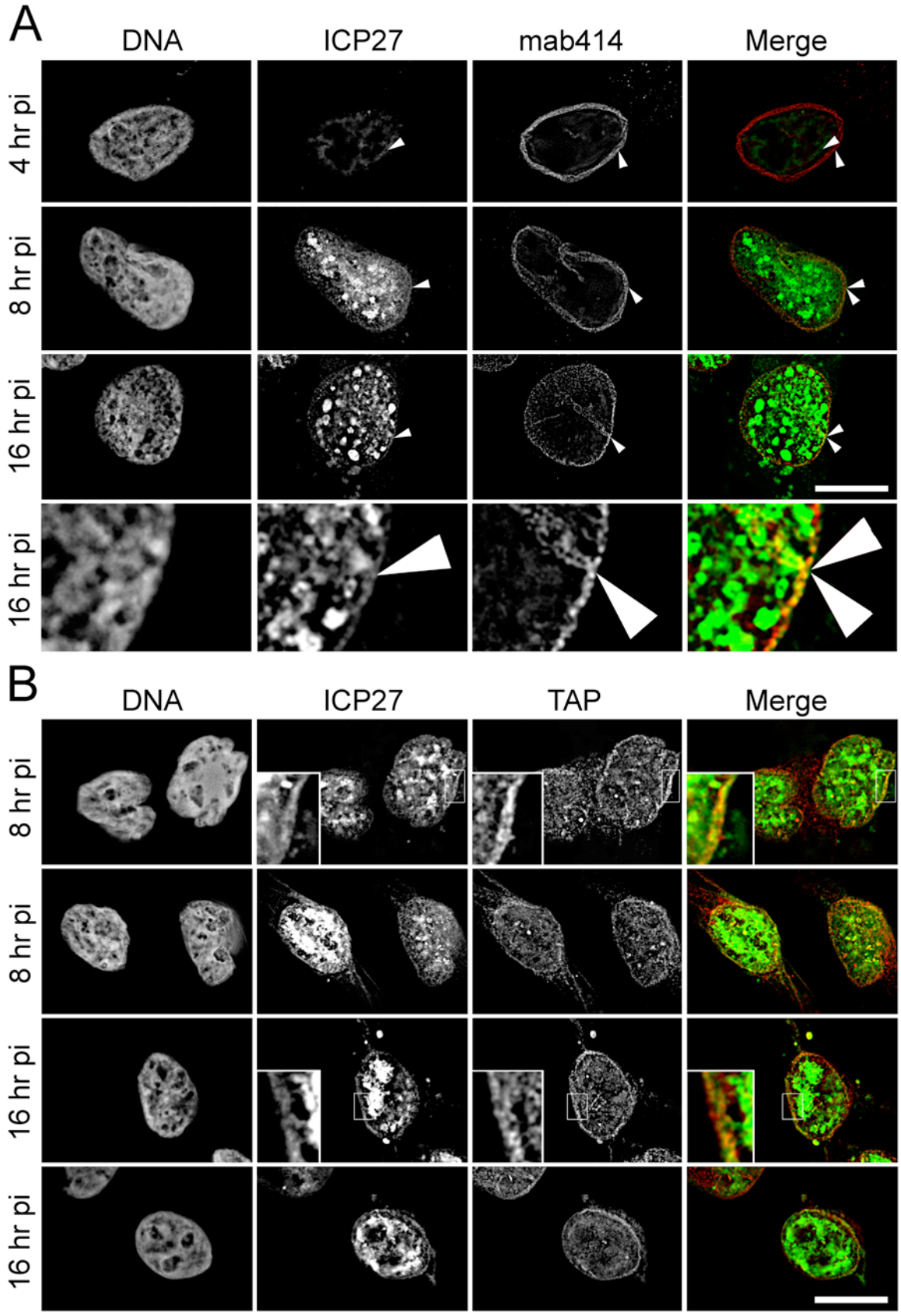
A
DNA
ICP27
mab414
Merge
4 hr pi
8 hr pi
16 hr pi
16 hr pi
B
DNA
ICP27
TAP
Merge
8 hr pi
8 hr pi
16 hr pi
16 hr pi

FIGURE 2

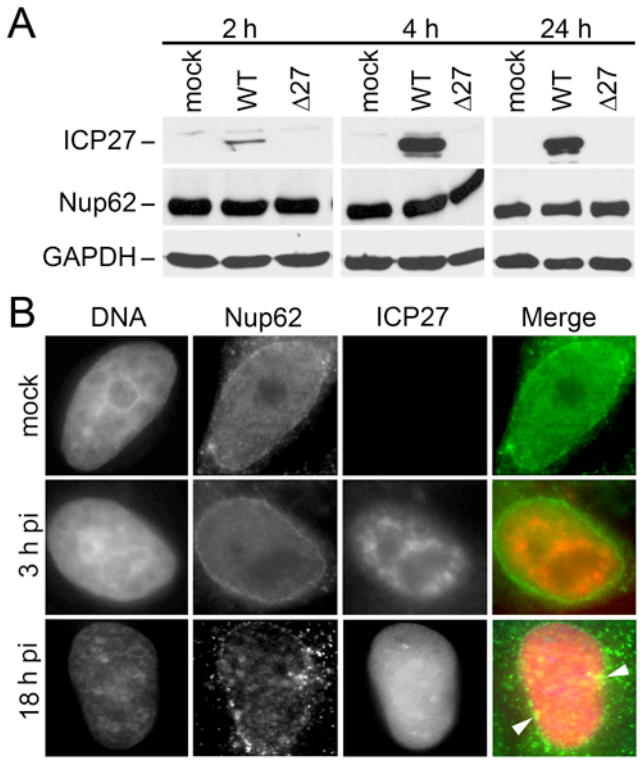
A
2 h
4 h
24 h
mock
WT
Δ27
mock
WT
Δ27
mock
WT
Δ27
ICP27 –
Nup62 –
GAPDH –
B
DNA
Nup62
ICP27
Merge
mock
3 h pi
18 h pi

FIGURE 3

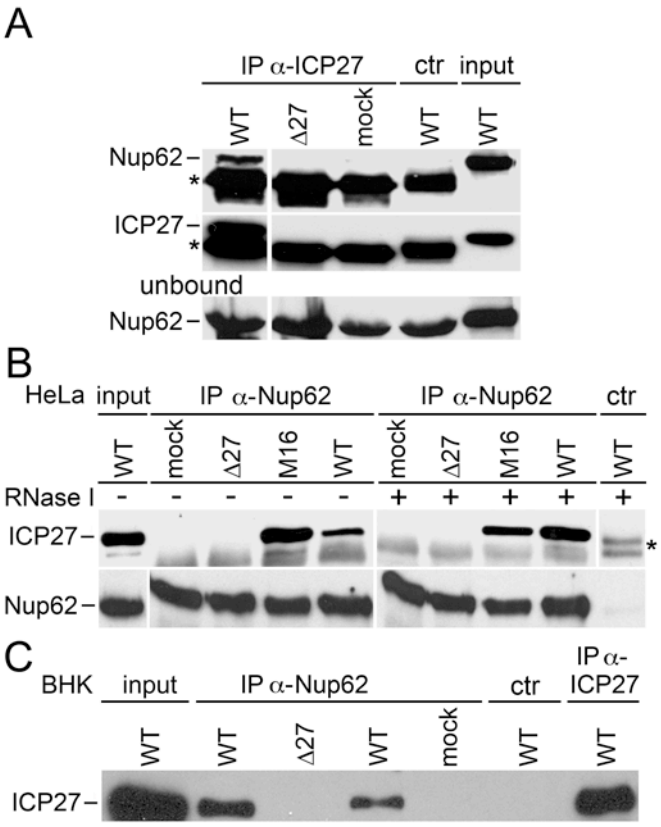
A
IP α-ICP27
ctr
input
WT
Δ27
mock
WT
WT
Nup62
*
ICP27
*
unbound
Nup62
B
HeLa
input
IP α-Nup62
IP α-Nup62
ctr
WT
mock
Δ27
M16
WT
mock
Δ27
M16
WT
WT
RNase I
- - - - - + + + + +
ICP27
*
Nup62
C
BHK
input
IP α-Nup62
ctr
IP α-ICP27
WT
WT
Δ27
WT
mock
WT
WT
ICP27

FIGURE 4

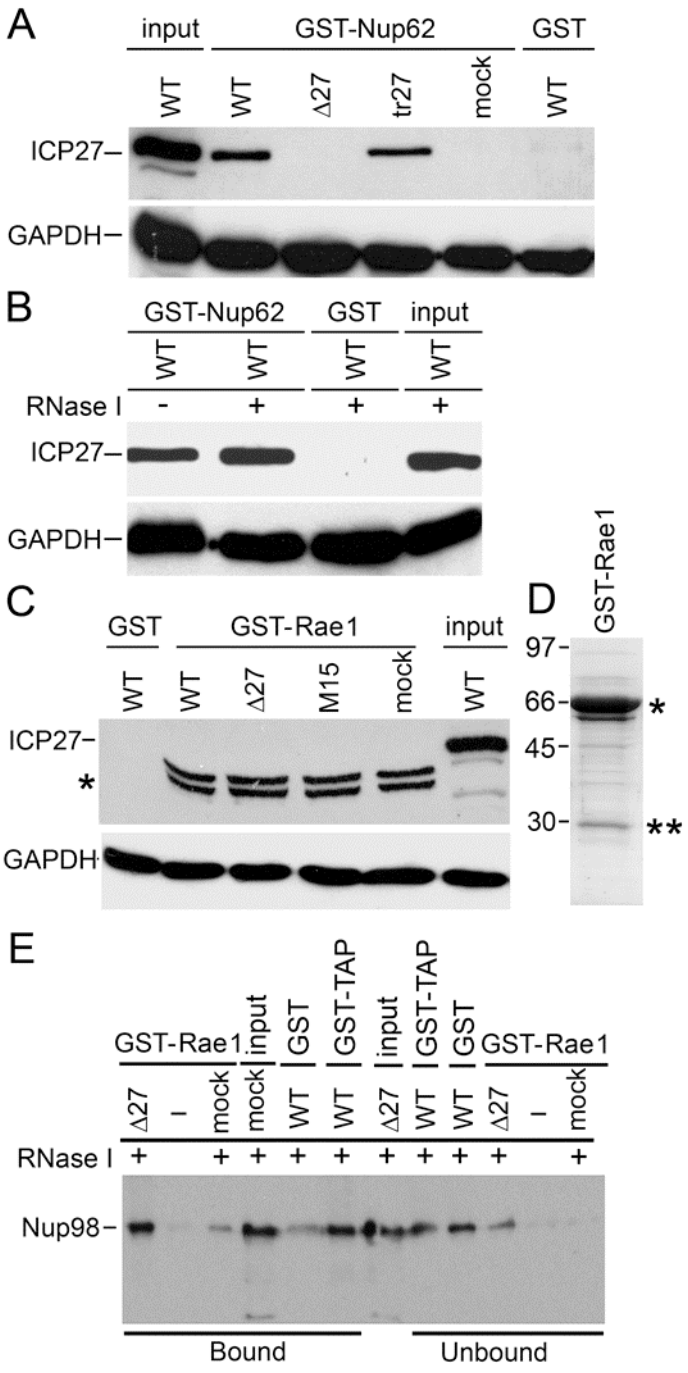
A
input
GST-Nup62
GST
WT
WT
Δ27
tr27
mock
WT
ICP27–
GAPDH–
B
GST-Nup62
GST
input
WT
WT
WT
WT
RNase I
-
+
+
+
ICP27–
GAPDH–
C
GST
GST-Rae1
input
WT
WT
Δ27
M15
mock
WT
ICP27–
*
GAPDH
D
GST-Rae1
97–
66–
45–
30–
*
**
E
GST-Rae1
input
GST
GST-TAP
input
GST-TAP
GST
GST-Rae1
Δ27
–
mock
mock
WT
WT
Δ27
WT
WT
Δ27
–
mock
RNase I
+
+
+
+
+
+
+
+
+
+
Nup98–
Bound
Unbound

FIGURE 5

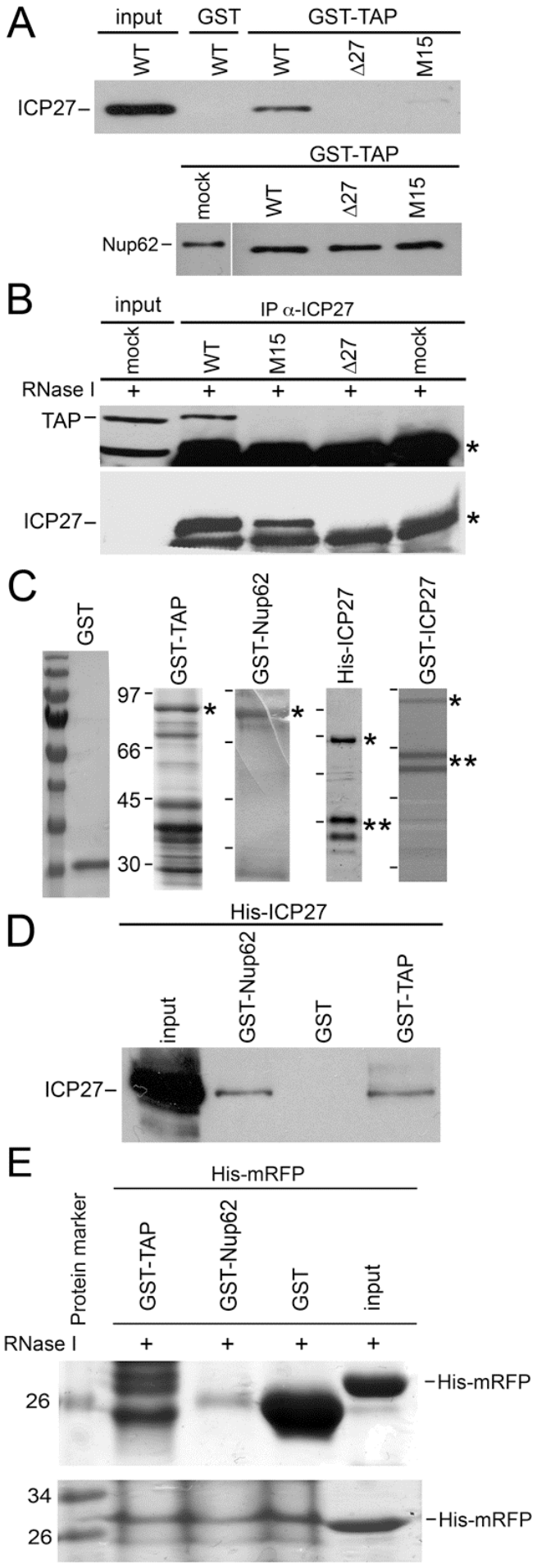
A
input
GST
GST-TAP
WT
WT
WT
Δ27
M15
ICP27–
GST-TAP
mock
WT
Δ27
M15
Nup62–
B
input
IP α-ICP27
mock
WT
M15
Δ27
mock
RNase I
+
+
+
+
+
TAP–
*
ICP27–
*
C
GST
GST-TAP
GST-Nup62
His-ICP27
GST-ICP27
97–
66–
45–
30–
*
*
*
*
**
*
**
D
His-ICP27
input
GST-Nup62
GST
GST-TAP
ICP27–
E
His-mRFP
Protein marker
GST-TAP
GST-Nup62
GST
input
RNase I
+
+
+
+
26
–His-mRFP
34
26
–His-mRFP

FIGURE 6

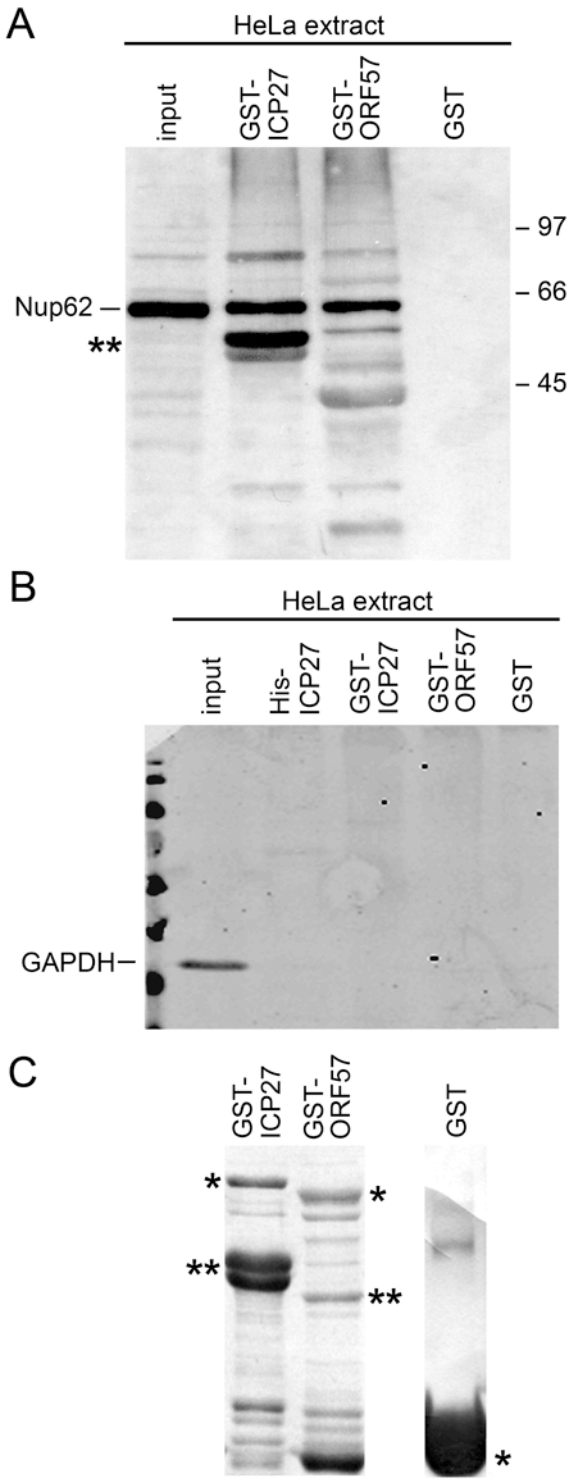
A
HeLa extract
input
GST-ICP27
GST-ORF57
GST
– 97
– 66
– 45
Nup62 –
**
B
HeLa extract
input
His-ICP27
GST-ICP27
GST-ORF57
GST
GAPDH–
C
GST-ICP27
GST-ORF57
GST
*
**
*
**
*

FIGURE 7

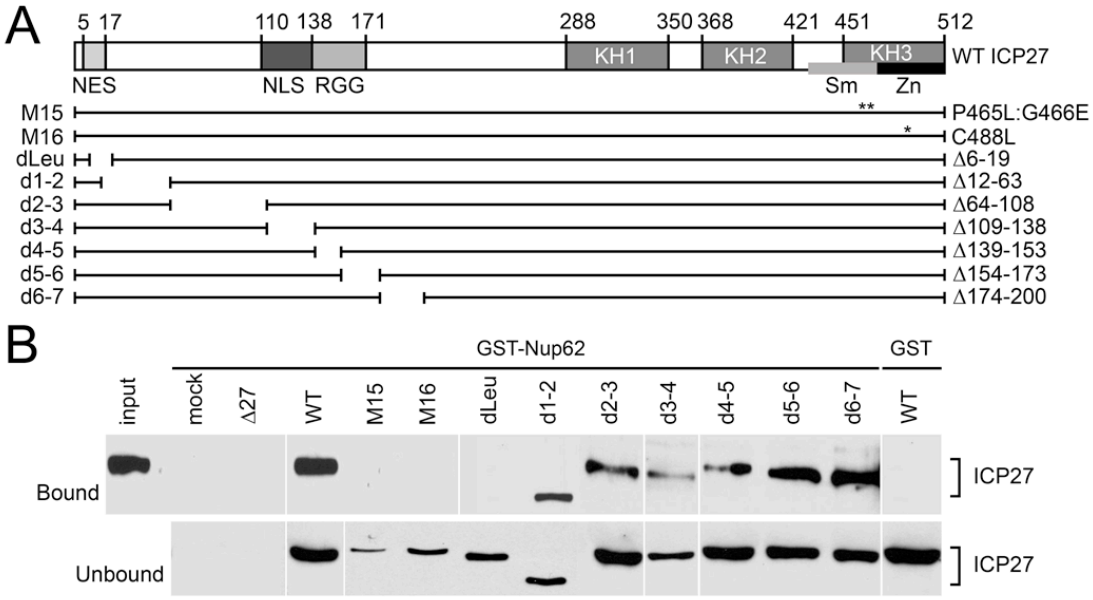
A
5 17
110 138 171
288
350 368
421
451
512
KH1
KH2
KH3
WT ICP27
NES
NLS RGG
Sm
Zn
M15
P465L:G466E
M16
C488L
dLeu
Δ6-19
d1-2
Δ12-63
d2-3
Δ64-108
d3-4
Δ109-138
d4-5
Δ139-153
d5-6
Δ154-173
d6-7
Δ174-200
B
GST-Nup62
GST
input
mock
Δ27
WT
M15
M16
dLeu
d1-2
d2-3
d3-4
d4-5
d5-6
d6-7
WT
Bound
Unbound
ICP27
ICP27

FIGURE 8

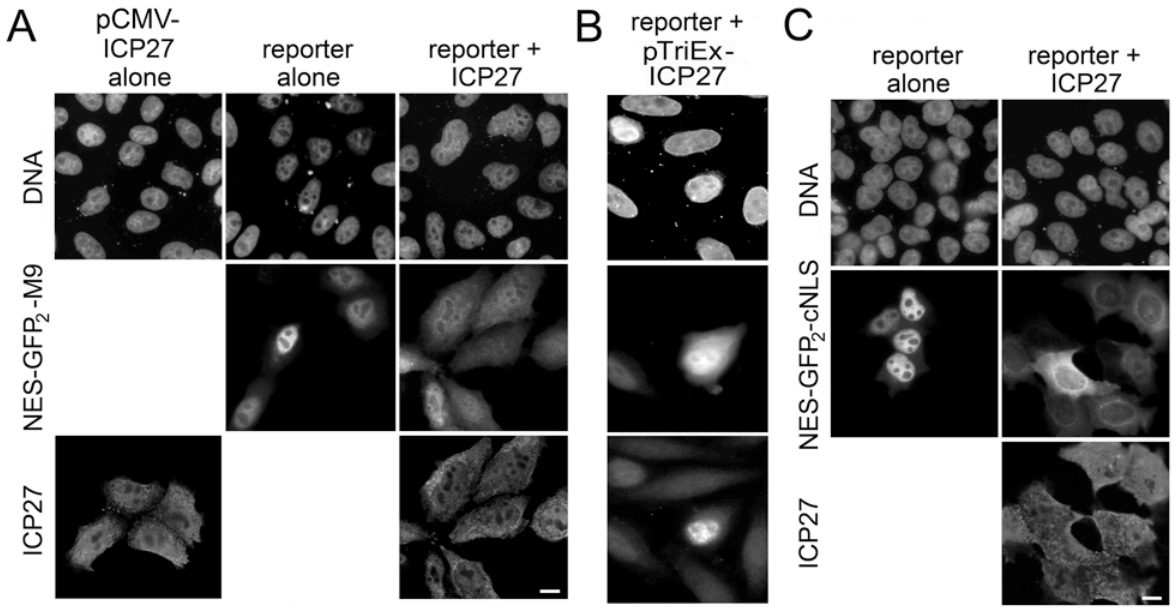
A
pCMV-ICP27 alone
reporter alone
reporter + ICP27
DNA
NES-GFP2-M9
ICP27
B
reporter + pTriEx-ICP27
C
reporter alone
reporter + ICP27
DNA
NES-GFP2-cNLS
ICP27

FIGURE 9

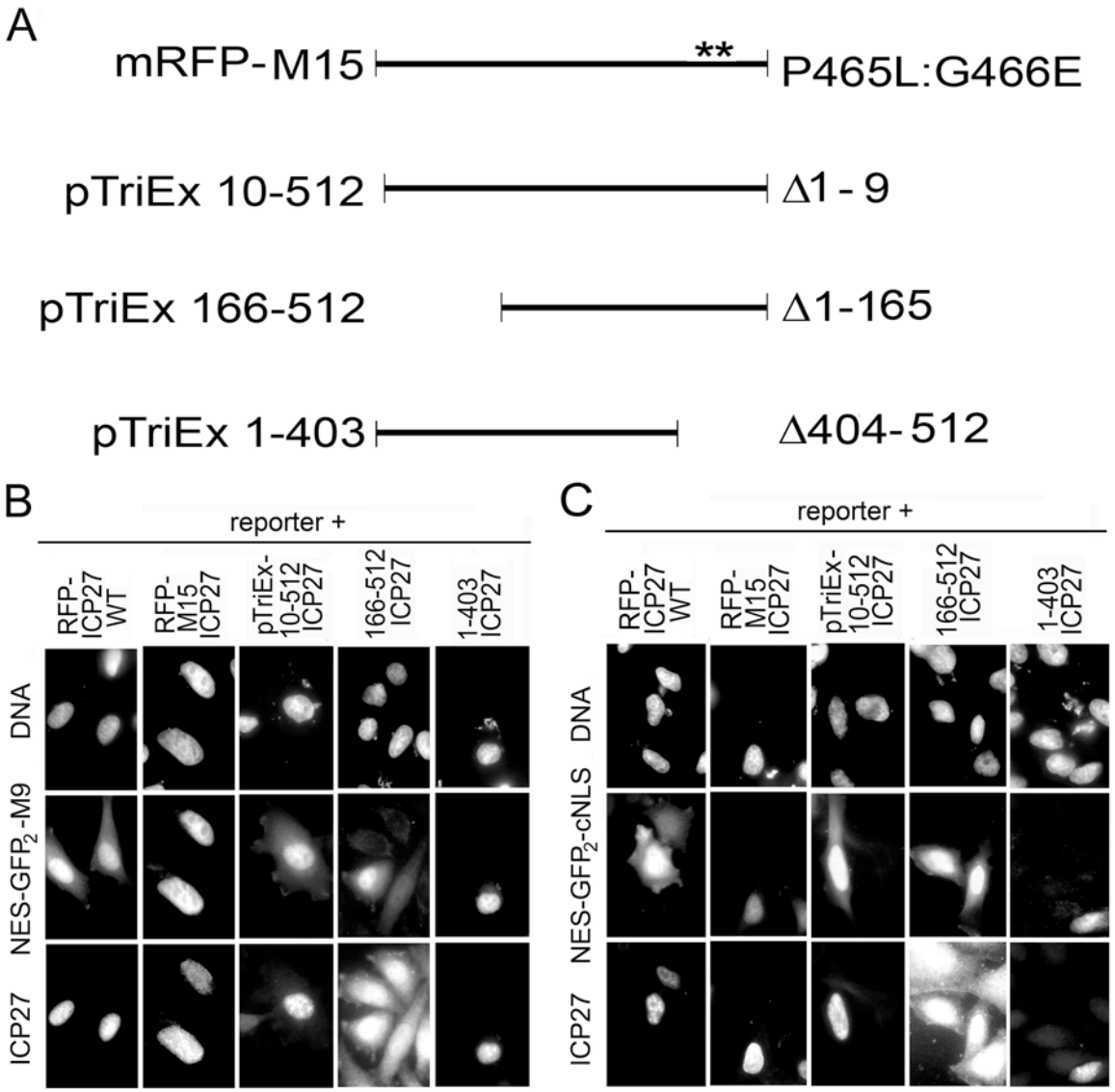
A
mRFP-M15
**
P465L:G466E
pTriEx 10-512
Δ1 - 9
pTriEx 166-512
Δ1-165
pTriEx 1-403
Δ404- 512
B
reporter +
RFP-ICP27 WT
RFP-M15 ICP27
pTriEx-10-512 ICP27
166-512 ICP27
1-403 ICP27
DNA
NES-GFP2-M9
ICP27
C
reporter +
RFP-ICP27 WT
RFP-M15 ICP27
pTriEx-10-512 ICP27
166-512 ICP27
1-403 ICP27
DNA
NES-GFP2-cNLS
ICP27